THE ASTRONOMICAL JOURNAL VOLUME 106, NUMBER 3 SEPTEMBER 1993

# LUMINOSITY FUNCTIONS AND COLOR–MAGNITUDE DIAGRAMS FOR THREE OB ASSOCIATIONS IN THE LARGE MAGELLANIC CLOUD

K. DEGIOIA-EASTWOOD[1]

Department of Physics and Astronomy, Northern Arizona University, Flagstaff, Arizona 86011-6010
Electronic mail: Kathy.Eastwood@nau.edu

R. P. MEYERS

6104 E. Duane Lane, Cave Creek, Arizona 85331

D. P. JONES

Space Telescope Science Institute, 3700 San Martin Drive, Baltimore, Maryland 21218
Electronic mail: djones@stsci.edu

*Received 1993 April 5; revised 1993 May 17*

## ABSTRACT

Using the point spread function photometry program DAOPHOT, we have used *UBV* CCD photometry to construct color–magnitude diagrams and luminosity functions for three OB associations in the Large Magellanic Cloud. The region LH 76 appears to be completely coeval; the region LH 13 shows some evidence for noncoevality which will need to be checked with spectra of the stars in question. The region LH 105, which lies on the southern edge of 30 Doradus, shows significant contamination by an underlying older population, possibly from previous star forming events. The luminosity functions, which serve as the first step toward determining the initial mass function in these regions, are calculated.

## 1. INTRODUCTION

This work is part of an ongoing study of stellar content of OB associations in the Magellanic Clouds. The ultimate goal is to determine the massive star content of the Clouds, determine the initial mass function (IMF) of massive star formation in individual regions and in each Cloud as a whole, and to relate the stellar content to the properties of the interstellar medium. These observations should contribute to our understanding of the star formation process in general and to understanding the factors which influence the IMF in particular.

The differences between our Galaxy and the Large Magellanic Cloud (LMC) make it important to compare star formation processes between the two galaxies. The LMC appears to be forming stars much more vigorously than our own Galaxy; there are more O3 stars in the LMC than have been found in the observable part of our Galaxy (Walborn 1986, and references within), and we see no complexes like 30 Doradus. The LMC also has a lower metallicity and a smaller dust-to-gas ratio than our Galaxy (Koornneef 1984; Dufour 1984, and many others). Very little is known about the dependence of the IMF on physical conditions such as the metallicity and dust-to-gas ratio out of which the stars are formed. Thus the LMC seems an ideal place to search for differences in the star formation process compared to our own galaxy.

In the first paper on this work, Massey *et al.* (1989, hereafter Paper I) determined the IMF for two adjacent OB associations in the LMC, LH 117 and 118 (Lucke & Hodge 1970). In Paper II, Massey *et al.* (1989) derived the IMF for NGC 346 in the Small Magellanic Cloud (SMC). In neither case was the IMF found to be significantly different than the high-mass IMF for the solar neighborhood as derived by Scalo (1986). However, Parker *et al.* (1992, Paper III) found that while LH 9 has a "normal" IMF, the slope for the IMF in LH 10 is significantly flatter, and several regions in our Galaxy have been found to have flatter mass functions (Massey & Thompson 1991; Massey & Johnson 1993). Also, the upper mass limit of the IMF has not been found to be different from that in our Galaxy in any of these regions, even though the metallicity in the SMC is down by a factor of almost 20 from that in the solar neighborhood (Massey 1993). This is in contradiction to theoretical predictions, which indicate that in regions of lower metallicity it ought to be possible to form stars of higher mass (e.g., Wolfire & Cassinelli 1986). It is clear that more work is needed to determine the slope and upper mass limit for a larger sample of star-forming regions. [It should be pointed out that the slope of the IMF in the solar neighborhood for the highest mass stars is in itself in dispute. See Scalo (1986) for an exhaustive review and a "best estimate."]

In this work we present color–magnitude diagrams and luminosity functions for LH 13, LH 76, and LH 105. The luminosity functions are a necessary first step toward the determination of the mass functions in these regions.

Massey (1985) has presented convincing arguments against the viability of constructing accurate mass functions for O stars using only *UBV* photometry. This is due

[1]Visiting Astronomer, Cerro Tololo Inter-american Observatory, National Optical Astronomy Observatory, National Optical Astronomy Observatories, operated by the Association of Universities for Research in Astronomy, Inc., under a cooperative agreement with the National Science Foundation.

 0004-6256/93/106(3)/1005/19/$0.90  

TABLE 1. Summary of observed fields.

| Field | $\alpha_{1975}$ | $\delta_{1975}$ | Date | Exposure Time (sec) | | |
|---|---|---|---|---|---|---|
| | | | | U | B | V |
| LH 13 | 04 57 39.0 | -66 29 22 | 26 Nov 85 | 700,150 | 120,20 | 120,20 |
| LH 76 | 05 32 26.0 | -67 41 58 | 29 Nov 85 | 700,150 | 120,20 | 120,20 |
| LH 105C | 05 40 11.0 | -69 46 29 | 2 Dec 85 | 150 | 20 | 20 |
| LH 105N | 05 40 10.0 | -69 44 37 | 2 Dec 85 | 150 | 20 | 20 |
| LH 105S | 05 40 11.0 | -69 47 30 | 2 Dec 85 | 150 | 20 | 20 |

to the degeneracy of visible colors for the hottest stars. This makes sense since the visible passbands all lie on the Rayleigh–Jeans tail of the spectral energy distribution, the slopes of which are very similar for high stellar temperatures. Even the UV continua of O stars are all very similar (Massa & Savage 1985). It is also true that the stars which are the brightest in the visible are not the most luminous, since the most luminous main-sequence stars emit most of their energy in the far ultraviolet. Thus IMFs for the regions studied here will have to wait for spectroscopy of the bluest stars.

The three regions were chosen primarily for their usefulness in calibrating the models of DeGioia-Eastwood (1992); they were among the regions chosen for that work because they were cleanly separated from neighboring regions in the infrared. These models attempt to determine the IMF of an unresolved region from observations of the radio, H$\alpha$, and infrared emission of the region. The LMC lies at an ideal distance for calibration of these models, since it lies at such a distance that stars can be resolved individually by ground-based telescopes, yet many of the H II regions can be observed as only slightly extended sources at radio and infrared wavelengths. Successful models of this type will eventually allow us to determine the IMF of unresolved regions in external galaxies.

## 2. OBSERVATIONS AND REDUCTIONS

### *2.1 The Data*

Images of the three regions were taken during 1985 November and December on the CTIO 0.9 m telescope with the RCA CCD (RCA4). The filters were standard Kitt Peak CCD U (UG2+liquid $CuSO_4$) and "Mould" interference *B* and *V*. The scale of the CCD frames was 0.49 arcsec/pixel, resulting in a field of view of $2.5 \times 4.0$ arcmin with the long axis oriented east–west. The frames were flattened using dome flats for all filters and additional twilight sky flats for *U* and *B*; the twilight sky was much closer to the color of our blue program stars than "el punto blanco."

The data consist of one field each for LH 76 and LH 13, and three overlapping frames running north–south for LH 105. The three frames overlapped so much that only the northern and southern frames are shown; the center frame is redundant. Both long and short exposures were taken for LH 13 and LH 76 in order to avoid saturation of the brightest stars. A list of the exposures which includes the coordinates of the centers, dates, and exposure times for all three regions is given in Table 1.

Representative individual frames are shown in Figs. 1–4 (Plates 43–46). North is to the left and east is at the bottom. In each case the longest exposure through the *V* filter is shown. In Figs. 3 and 4 we show the northern and southern frames for LH 105. In all these figures, the stars for which we have new photometry are marked with white dots. Note that DAOPHOT was not able to successfully resolve every clump of stars and nebulosity; there are a few clumps for which we have no acceptable photometry.

### *2.2 The Photometry*

Observations of Landolt's (1983) standard stars were done seven to ten times per night using five to seven stars, with a total of approximately 300 observations over nine nights. Since our program objects were primarily blue stars, we limited ourselves to fairly blue standards. The determination of the extinction and transformation equations are discussed in great detail in Paper I. Since we are interested primarily in the blue stars, the transformation coefficients were intentionally optimized for the color range $B-V<0.0$ and $U-B<0.0$.

The photometry was performed using the IRAF version of the crowded-field photometry program DAOPHOT, written by Stetson (1987). The final fitting was done using the ALLSTAR routine rather than NSTAR. Great care was taken to accurately match observations of stars between frames through different filters, between long and short exposures, and between overlapping frames. Where there were multiple observations of a star, the magnitudes were obtained by doing a weighted average according to the uncertainties in the magnitudes (as produced by DAOPHOT).

With DAOPHOT, the user defines an empirical point spread function (PSF) for each frame by averaging the cleanest, brightest stars. On some frames the very brightest stars were not suitable for PSF stars due to saturation, overcrowding, or bad pixels. Thus in these cases ALLSTAR attempted to fit some stars brighter than those used to define the PSF. In these cases the uncertainties are higher. When the nebulosity was extremely heavy, an iterative process suggested by Parker (1991) was used to determine the magnitudes for the stars embedded in the nebulosity.

The standards were measured through an aperture with a 15 pixel aperture, while the DAOPHOT magnitudes were tied to an aperture with a 3 pixel radius. Thus for each frame it was necessary to determine an aperture correction

from the 3 pixel aperture to the 15 pixel aperture. This aperture correction was derived by averaging a "curve of growth" for the brightest isolated stars in the frame. The aperture correction is most likely the largest source of photometric error. In the shorter exposures fewer stars had photon statistics sufficient to determine an aperture correction. This fact, combined with the problem of the brightest stars sometimes being brighter than the PSF stars, leads to the brightest stars having disproportionately large errors in their photometry.

Since the purpose of the photometry was to determine a luminosity function, we ran the CCDCAL software (originally written by Peter Stetson) twice: one for each set of *UBV* frames, and again for just the *B* and *V* frames. This picked up many more stars which were too faint and too red to produce a reliable magnitude on the *U* frame.

DAOPHOT calculates internal uncertainties which include the CCD read noise, the sky noise, the photon statistics, and an estimate of how well the PSF was fit to the individual star. In Figs. 5, 6, and 7 we have plotted the internal uncertainties in $V$, $B-V$, and $U-B$ as a function of $V$ magnitude for each region. The apparent bifurcation of the uncertainties in some plots is probably due to the fact that some stars were measured twice, which reduced the uncertainties, and some were only measured once. In Table 2 we list the median errors for each region for half-magnitude bins. Stars brighter than the brightest bin or fainter than the faintest bin listed belong in the bin closest to its magnitude; this was done so that each bin had enough stars for a reasonable average. Note that the uncertainties for LH 105 are much greater than for the other two regions; this is directly attributable to the fact that the seeing was much worse for these observations than for the other two regions. In addition, no deep exposures were taken of LH 105.

In Tables 3 through 6 we present the photometry for the three regions. The northern and southern regions of LH 105 are listed in separate tables; the coordinates in Table 5 refer to the image in Fig. 3, and the coordinates in Table 6 refer to the image in Fig. 4. The stars are numbered in order of increasing right ascension, which is increasing $Y$. The $X$ and $Y$ coordinates given for the centers of the stars are in pixels, measured from the upper left corner of the frame. The stars can be identified by their coordinates in pixels in Figs. 2 through 5, remembering that the total frame is 316 pixels wide in $X$ and 500 pixels high in $Y$. There are a very few stars which are just barely off the frames shown; this occurred when the short $V$ exposure was slightly offset from the long one, and a magnitude was picked up off the short frame. Thus these stars do not show up in the images, which are the long $V$ exposures.

In keeping with Paper I and Paper II, in Tables 3 through 6 we denote with a colon those magnitudes or colors having an uncertainty more than twice as large as the median values presented in Table 2, or a color which is outside the color range for which our photometric transformations are optimized, or a star which had a chi value calculated by DAOPHOT to be more than 2.0 (which indicates a bad fit to the PSF). We denote with two colons a

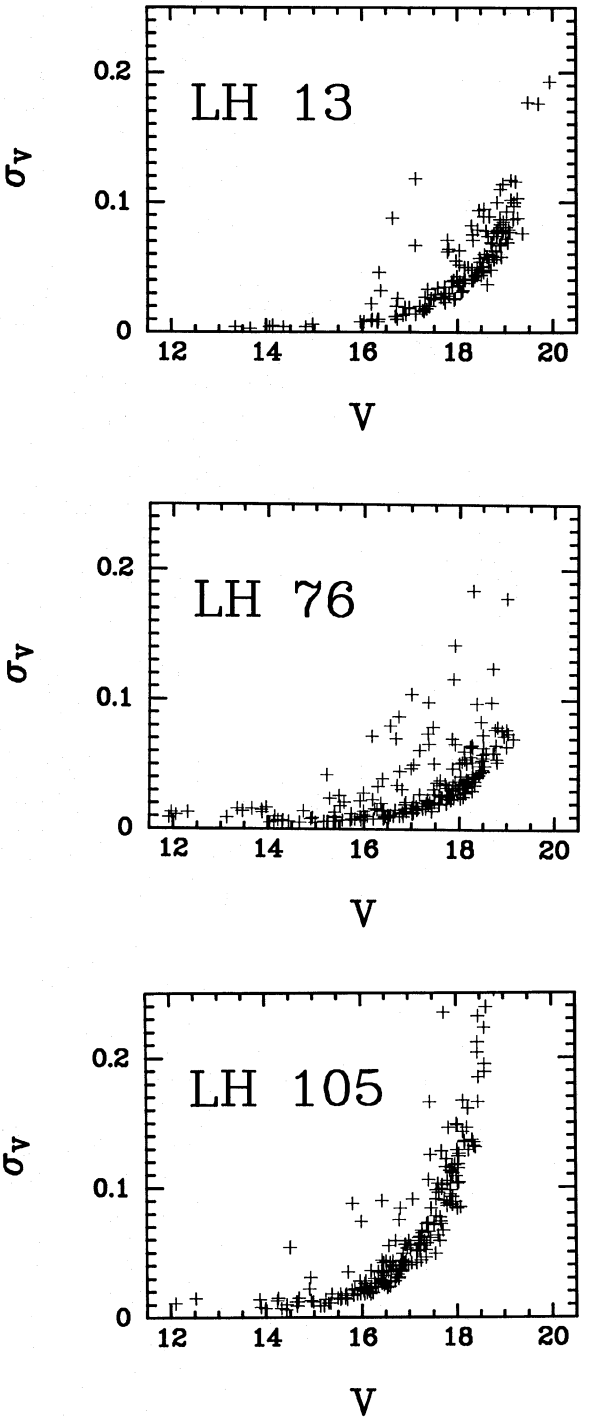


FIG. 5. The internal uncertainties in the $V$ magnitude as a function of $V$ magnitude for the three regions.

magnitude or color with an uncertainty greater than three times the median values in Table 2. Many of the worst uncertainties can be traced to a star being close to the edge of a frame, or being near a saturated star.

Several of the brightest stars were too saturated or too crowded, even on the short frames, for ALLSTAR to be able to make a good fit. Three of these stars are in the list of

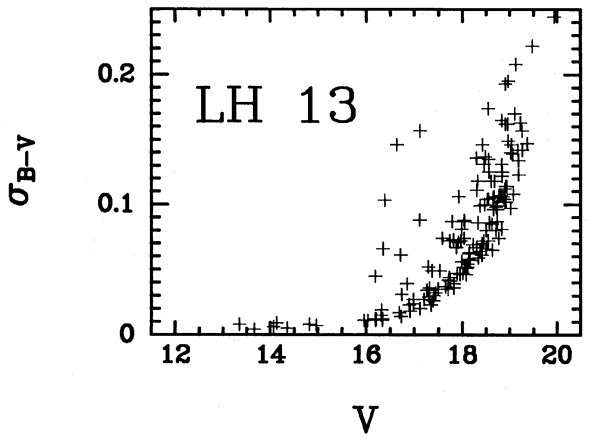


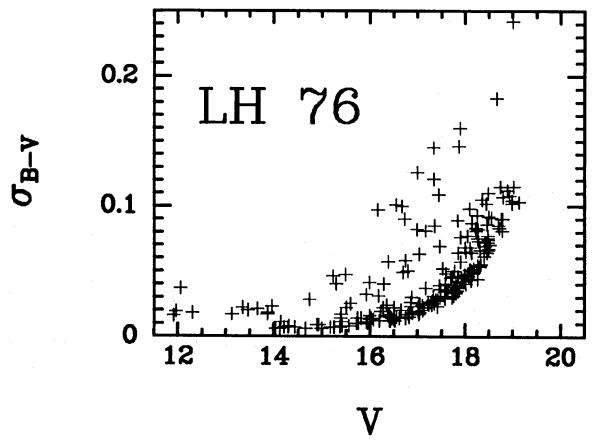


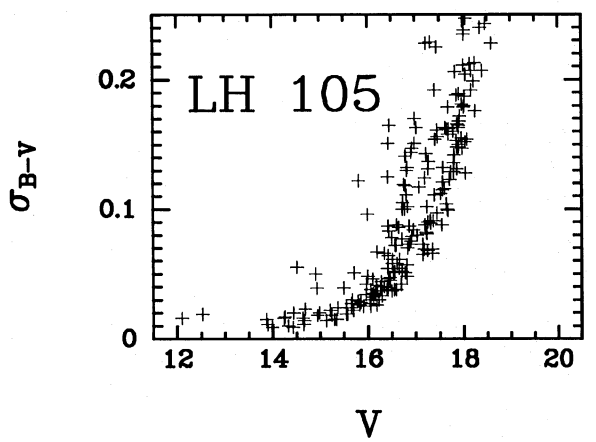


FIG. 6. The internal uncertainties in the $B-V$ color as a function of $V$ magnitude for the three regions.

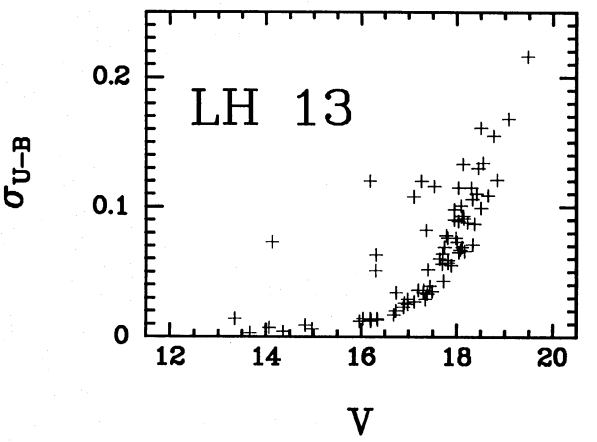


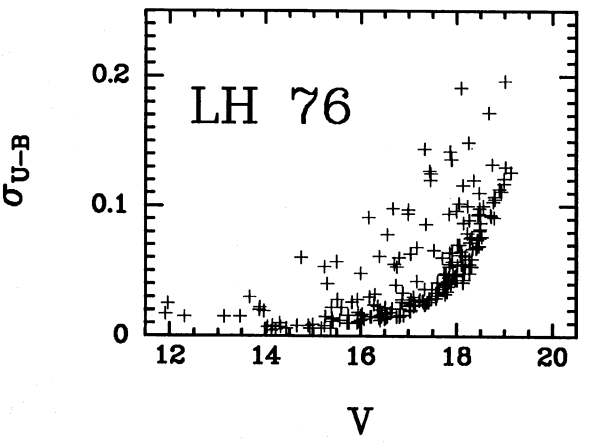


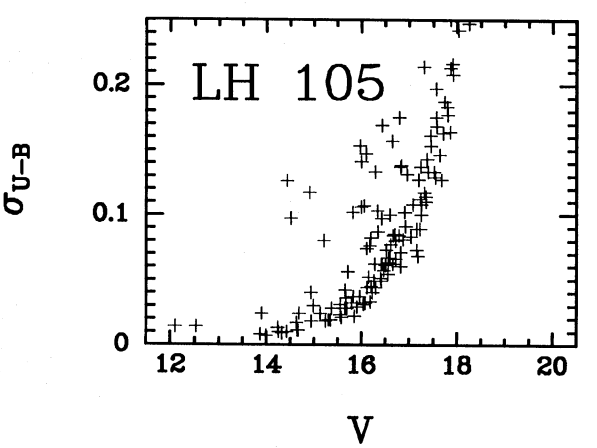


FIG. 7. The internal uncertainties in the $U-B$ color as a function of $V$ magnitude for the three regions.

Sanduleak (1969), and their photometry is available from different sources and compiled in Rousseau *et al.* (1978). As discussed later, we have added these three stars into the color–magnitude diagrams and luminosity functions derived here, but they are not included in the tables of photometry. Two of these stars are in LH 76; SK-67 173 is at approximate coordinates 75, 135, and SK-67 178a is at approximate coordinates 255, 298. The third star, SK-66 41, is in LH 13 at approximate coordinates 101, 296.

We were lucky enough to have two sources of photometry with which to compare ours. In his Ph.D. thesis, Lucke (1972) obtained photographic $BV$ photometry for LH 76. The OB association LH 105 contains the x-ray source LMC X-1, which has stimulated considerable inter-

TABLE 2. Median photometric errors in half-magnitude bins.

| | LH 13 | | | LH 76 | | | LH 105 | | |
|---|---|---|---|---|---|---|---|---|---|
| Bin Center | $\sigma_V$ | $\sigma_{B-V}$ | $\sigma_{U-B}$ | $\sigma_V$ | $\sigma_{B-V}$ | $\sigma_{U-B}$ | $\sigma_V$ | $\sigma_{B-V}$ | $\sigma_{U-B}$ |
| <15.50 | | | | 0.009 | 0.011 | 0.011 | 0.012 | 0.016 | 0.018 |
| 15.75 | | | | 0.010 | 0.014 | 0.016 | 0.018 | 0.028 | 0.036 |
| 16.25 | | | | 0.014 | 0.016 | 0.017 | 0.026 | 0.040 | 0.059 |
| 16.75 | 0.010 | 0.014 | 0.014 | 0.015 | 0.023 | 0.024 | 0.039 | 0.078 | 0.080 |
| 17.25 | 0.020 | 0.033 | 0.036 | 0.019 | 0.027 | 0.027 | 0.058 | 0.106 | 0.112 |
| 17.75 | 0.032 | 0.053 | 0.069 | 0.027 | 0.039 | 0.042 | 0.097 | 0.157 | 0.185 |
| 18.25 | 0.044 | 0.069 | 0.091 | 0.052 | 0.075 | 0.087 | 0.137 | 0.236 | 0.253 |
| >18.50 | 0.077 | 0.118 | 0.145 | | | | | | |

est. Dufour & Duval (1975) obtained photoelectric *UBV* photometry for several of the stars in the region. In Table 7 we present cross identifications between our stars and the numbering systems of Lucke, Dufour and Duval, Sanduleak (1969), Cowley *et al.* (1978), Feast *et al.* (1960), and the *HST Guide Star Catalog* (1992). In LH 13 and LH 76 there were enough stars from the *Guide Star Catalog* for us to be able to derive accurate coordinates for the stars; these coordinates are given in Table 7. However, in LH 105 there were not enough stars from the *Guide Star Catalog* in the field for us to be certain of their identification, nor to derive coordinates.

In Fig. 8 we present graphically the comparison of our photometry to that of Lucke (1972) and Dufour & Duval (1975), plotted as the difference in magnitudes in the sense of our photometry minus their photometry. The crosses represent Lucke's photographic iris photometry, and the circles represent Dufour's photoelectric photometry. Only Lucke's "good" magnitudes have been included, i.e., no multiple or saturated stars, and only stars without colons in Tables 3 through 6 have been included. The agreement in $V$ magnitude is excellent in both cases over a wide range in magnitude. Our magnitudes might be slightly fainter than Dufour and Duval's, but there are not enough data points to tell for sure. As noted in Paper I, there appears to be a systematic difference between our $B-V$ colors and Lucke's in the sense that our photometry is redder. However, no such difference is seen between our photometry and Dufour and Duval's. The agreement between our $U-B$ colors and those of Dufour and Duval is also excellent. (We note here a difference of almost precisely two magnitudes between our $V$ magnitude and Dufour and Duval's for their star number 8. Since our colors for that star match his within several hundredths, as do the $V$ magnitudes for the other stars in common, we suspect that his $V$ magnitude is in typographical error and that it should be 14.23 instead of 12.23.)

## 3. ANALYSIS

### *3.1 The Reddening Correction*

The reddening for each region was determined by calculating the reddening-free index $Q=(U-B)-0.72(B-V)$ for the bluest stars, i.e., those stars with an intrinsic $B-V$ less than zero. First the stars were plotted on a color–color diagram to get a rough idea of the reddening. The diagrams are presented in Fig. 9; only stars with errors less than 0.07 mag are shown. There is obviously scatter in the reddening values, indicating differential reddening across the clusters, particularly in LH 105 which has the largest and most variable reddening. The $Q$ values were then calculated for all stars that appear in Fig. 9. The average reddening for each cluster was determined by averaging the $E(B-V)$ values calculated from the $Q$ values for these stars. Stars with individual $Q$ values were dereddened using their own $Q$ value, and the remaining stars were dereddened using the median reddening for each region. The median was felt to be more appropriate than the mean since a few high values for the reddening in dusty regions would skew the distribution.

The median, mean, and standard deviation of the color excess $E(B-V)$ are presented in Table 8 for all three regions, as well as the number of stars used in the calculations. Note that in each case the standard deviation is significant and that the mean is higher than the median, indicating that the reddening is highly variable and that some of the stars are quite highly reddened. The reddening is similar in LH 13 and LH 76, but significantly higher in LH 105.

### *3.2 The Color–Magnitude Diagrams*

In Fig. 10 we present dereddened color–magnitude diagrams in $V$ vs $B-V$ for the three regions, and in Fig. 11 the dereddened $V$ vs $U-B$ diagrams. In keeping with Paper I and Paper II, we have plotted stars with "good" photometry, i.e., those stars with uncertainties in both magnitudes and colors less than 0.07 mag, as circles. The remaining stars are plotted as crosses. In Fig. 11 we can see that not much extra information has been gained by using the $U-B$ color for the color–magnitude diagram; spectra are still necessary to distinguish the temperatures of the hottest stars.

As discussed above, we have added to Figs. 10 through 13 three stars which do not appear on our photometry lists. These three stars were inside our frames, but due to saturation and nebulosity, ALLSTAR was unable to fit them successfully. The stars are SK-67 178a and SK-67 173 in LH 76, and SK-66 41 in LH 13 (Sanduleak 1969). For the sake of completeness we have added these stars into the

TABLE 3. Photometry for stars in the region LH 13.

| Star | X | Y | V | B−V | U−B | Star | X | Y | V | B−V | U−B | Star | X | Y | V | B−V | U−B |
|---|---|---|---|---|---|---|---|---|---|---|---|---|---|---|---|---|---|
| 1 | 62.8 | 5.5 | 18.84 | 0.43 | | 41 | 10.8 | 164.1 | 19.36 | 0.12 : | | 81 | 238.4 | 275.9 | 18.57 | 0.19 | |
| 2 | 172.9 | 8.5 | 18.17 | −0.02 | −0.44 | 42 | 157.5 | 164.8 | 17.40 | −0.12 | −0.68 | 82 | 169.6 | 276.8 | 17.89 | −0.07 | −0.63 |
| 3 | 235.9 | 11.7 | 18.94 | −0.11 | | 43 | 284.3 | 171.6 | 19.02 | −0.05 | | 83 | 91.1 | 277.4 | 18.04: | 0.25 : | 0.03 : |
| 4 | 117.3 | 16.4 | 17.73 | −0.16 | −0.67 | 44 | 266.0 | 172.2 | 19.19: | −0.54 | | 84 | 73.2 | 281.6 | 18.83: | −0.12 | −0.63 |
| 5 | 56.0 | 17.3 | 17.29: | 1.45 : | | 45 | 181.2 | 177.5 | 18.11 | 0.05 | −0.38 | 85 | 81.9 | 281.6 | 16.89 | −0.03 | −0.63 |
| 6 | 32.6 | 24.5 | 19.06 | 0.43 : | | 46 | 169.6 | 182.7 | 19.12: | 0.81 :: | | 86 | 229.3 | 283.5 | 18.67: | −0.17 | |
| 7 | 7.8 | 29.1 | 18.63 | −0.14 | | 47 | 174.1 | 202.4 | 19.18 | −0.09 | | 87 | 115.5 | 286.1 | 18.30 | 0.30 | |
| 8 | 134.4 | 31.6 | 17.87: | 1.03 : | | 48 | 168.7 | 202.7 | 18.81 | 0.23 | | 88 | 220.1 | 286.9 | 18.56: | −0.04 | |
| 9 | 109.2 | 41.9 | 17.65 | 0.03 | −0.31 | 49 | 163.2 | 211.9 | 18.66: | 0.76 : | | 89 | 120.6 | 287.0 | 18.45: | 0.04 | |
| 10 | 56.0 | 44.3 | 16.85: | 1.35 : | | 50 | 143.7 | 212.4 | 19.26: | 0.03 : | | 90 | 252.6 | 287.1 | 19.94:: | −0.44 :: | |
| 11 | 290.1 | 49.3 | 18.30: | 1.04 : | | 51 | 269.9 | 212.6 | 13.35: | 0.71 : | 0.29 : | 91 | 157.4 | 290.1 | 18.76 | 0.02 | −0.57 |
| 12 | 221.6 | 56.9 | 17.20 | −0.02 | −0.58 | 52 | 84.4 | 218.1 | 17.37: | 0.57 : | −0.27 : | 92 | 60.7 | 291.2 | 18.60 | 0.20 | |
| 13 | 100.5 | 64.0 | 17.73: | 1.41 : | | 53 | 191.9 | 220.6 | 18.96 | 0.27 : | | 93 | 165.7 | 295.0 | 19.07 | 0.06 | −0.76 |
| 14 | 287.6 | 76.0 | 16.03 | 0.01 | −0.77 | 54 | 241.4 | 225.3 | 18.14 | 0.02 | −0.30 | 94 | 202.6 | 296.4 | 16.72: | 1.02 : | |
| 15 | 115.4 | 76.8 | 18.08 | 0.20 | −0.13 | 55 | 105.7 | 231.6 | 18.41 | 0.01 | −0.45 | 95 | 91.6 | 299.7 | 17.12:: | −0.04 :: | |
| 16 | 310.5 | 78.9 | 17.92: | 1.03 : | | 56 | 101.0 | 233.9 | 18.88 | 0.28 | | 96 | 294.4 | 305.9 | 18.15 | −0.14 | −0.68 |
| 17 | 300.4 | 81.9 | 16.74 | −0.16 | −0.75 | 57 | 84.8 | 235.4 | 18.46: | 0.63 : | | 97 | 131.4 | 307.7 | 13.66 | −0.14 | −1.07 |
| 18 | 98.2 | 84.7 | 17.31 | 0.01 | −0.25 | 58 | 284.0 | 238.2 | 19.10: | 0.55 : | | 98 | 36.9 | 308.5 | 18.01 | −0.08 | −0.28 |
| 19 | 301.1 | 85.6 | 14.14: | 1.74 : | 1.71 : | 59 | 24.1 | 244.3 | 18.54 | 0.17 | −0.29 | 99 | 140.6 | 308.6 | 17.82 | −0.25 | −0.35 |
| 20 | 196.5 | 88.8 | 18.73 | −0.09 | | 60 | 304.5 | 248.6 | 18.83 | −0.09 | | 100 | 115.8 | 308.9 | 17.78 | −0.15 | |
| 21 | 279.4 | 89.8 | 17.92: | 1.57 : | | 61 | 248.4 | 248.9 | 16.31: | 0.72 : | 0.30 : | 101 | 87.9 | 309.5 | 18.64 | −0.08 | −1.06 |
| 22 | 235.6 | 95.6 | 16.34 | −0.13 | −0.64 | 62 | 72.5 | 251.9 | 14.35 | −0.14 | −0.95 | 102 | 93.7 | 310.6 | 16.98 | −0.12 | −0.92 |
| 23 | 57.9 | 101.8 | 17.41 | 0.00 | −0.46 | 63 | 95.7 | 253.3 | 16.34 | −0.15 | −0.89 | 103 | 109.8 | 314.7 | 18.04 | −0.03 | −1.00 |
| 24 | 54.0 | 104.3 | 18.13 | 0.03 | −0.34 | 64 | 26.3 | 255.6 | 18.42: | 0.98 : | | 104 | 23.2 | 315.2 | 19.26 | 0.17 : | |
| 25 | 30.5 | 106.1 | 18.92 | 0.13 | | 65 | 303.9 | 256.1 | 18.50: | 0.13 : | 0.01 : | 105 | 139.9 | 318.9 | 17.78: | 0.11 | −0.93 |
| 26 | 41.9 | 115.2 | 18.97: | 0.87 : | | 66 | 133.7 | 256.2 | 18.44 | −0.04 | −0.32 | 106 | 107.7 | 319.2 | 18.90: | −0.09 : | |
| 27 | 130.1 | 124.0 | 17.58: | 0.95 : | | 67 | 99.7 | 260.2 | 17.32 | 0.00 | −0.72 | 107 | 227.7 | 320.2 | 19.17 | 0.49 : | |
| 28 | 55.2 | 124.4 | 18.37 | −0.05 | −0.67 | 68 | 68.9 | 260.6 | 18.32 | 0.00 | 0.25 | 108 | 126.2 | 321.2 | 16.98 | −0.15 | −0.99 |
| 29 | 269.3 | 127.3 | 17.99: | −0.20 : | −0.03 : | 69 | 176.3 | 261.2 | 18.33 | −0.10 | −0.85 | 109 | 62.8 | 323.0 | 16.69 | −0.12 | −0.82 |
| 30 | 66.3 | 128.6 | 15.96 | 0.16 | −0.78 | 70 | 25.2 | 263.7 | 18.90: | 1.20 : | | 110 | 167.6 | 324.1 | 19.12: | 1.73 :: | |
| 31 | 305.0 | 129.7 | 17.95 | −0.08 | 0.06 | 71 | 236.1 | 265.7 | 18.05 | −0.11 | −0.46 | 111 | 286.8 | 325.2 | 16.73 | −0.12 | −0.81 |
| 32 | 197.2 | 137.1 | 19.03: | 0.19 : | | 72 | 89.7 | 265.9 | 16.19 | −0.08 | −0.82 | 112 | 243.7 | 325.6 | 18.50 | 0.16 | −1.00 |
| 33 | 121.6 | 139.6 | 18.82 | 0.45 | | 73 | 36.3 | 266.5 | 19.48:: | 0.15 :: | −0.92 : | 113 | 263.8 | 326.2 | 17.71 | 0.09 | −0.31 |
| 34 | 325.2 | 143.8 | 17.11:: | −0.09 : | −0.82 :: | 74 | 197.8 | 268.7 | 16.19: | 0.79 : | 0.92 :: | 114 | 201.1 | 326.7 | 14.96 | −0.13 | −0.94 |
| 35 | 24.2 | 146.2 | 16.91 | 0.00 | −0.74 | 75 | 191.9 | 270.4 | 17.96 | 0.11 | 0.84 :: | 115 | 117.0 | 328.4 | 17.50 | −0.08 | −0.90 |
| 36 | 190.5 | 152.0 | 18.08 | −0.05 | −0.64 | 76 | 203.3 | 272.0 | 16.64:: | 0.21 :: | | 116 | 73.8 | 331.6 | 18.30 | −0.01 | −0.24 |
| 37 | 208.2 | 152.7 | 19.19: | 0.02 | | 77 | 101.3 | 272.2 | 16.21 | −0.07 | −0.79 | 117 | 85.4 | 332.3 | 14.07: | 0.60 : | 0.31 : |
| 38 | 134.1 | 156.6 | 18.70 | −0.09 | | 78 | 254.5 | 274.0 | 19.22: | 0.05 : | | 118 | 235.6 | 341.8 | 14.82 | 0.46 | −0.88 |
| 39 | 321.3 | 163.9 | 16.36: | 0.90 : | | 79 | 230.0 | 274.1 | 17.75 | 0.07 | −0.11 | 119 | 305.3 | 344.2 | 17.82 | −0.19 | −0.27 |
| 40 | 106.4 | 164.1 | 18.55: | 1.04 : | | 80 | 120.8 | 275.5 | 18.77 | −0.31 | | 120 | 177.2 | 344.2 | 18.95: | 0.25 : | |

TABLE 3. (continued)

| Star | X | Y | V | B−V | U−B | Star | X | Y | V | B−V | U−B | Star | X | Y | V | B−V | U−B |
|---|---|---|---|---|---|---|---|---|---|---|---|---|---|---|---|---|---|
| 121 | 123.7 | 351.2 | 19.70:: | 0.14 :: | | 136 | 129.8 | 416.3 | 18.52: | 1.02 : | | 151 | 26.8 | 481.1 | 18.91 | 0.05 | |
| 122 | 53.3 | 354.9 | 18.70 | −0.02 | | 137 | 25.9 | 417.2 | 17.95 | 0.14 | 0.20 | 152 | 67.5 | 493.0 | 18.37: | 1.19 : | |
| 123 | 128.3 | 362.8 | 17.44 | −0.04 | −0.90 | 138 | 306.5 | 417.8 | 17.12 | −0.10 | −0.71 | 153 | 73.2 | 494.1 | 18.90 | 0.05 | |
| 124 | 276.5 | 362.9 | 18.73 | 0.14 | | 139 | 186.5 | 420.5 | 16.20 | −0.10 | −0.92 | 154 | 53.0 | 496.9 | 18.04: | 0.92 : | |
| 125 | 212.7 | 366.7 | 17.98: | 0.94 : | | 140 | 138.1 | 425.5 | 18.65 | 0.41 | | | | | | | |
| 126 | 273.2 | 377.9 | 18.48: | 1.09 : | | 141 | 130.4 | 425.7 | 18.82: | 1.05 : | | | | | | | |
| 127 | 264.3 | 381.0 | 18.22 | −0.18 | −0.59 | 142 | 133.2 | 434.3 | 18.32: | 0.93 : | | | | | | | |
| 128 | 226.4 | 382.2 | 17.53: | 0.57 : | 0.35 : | 143 | 245.1 | 440.1 | 18.42 | 0.11 | | | | | | | |
| 129 | 106.0 | 391.8 | 17.35 | −0.03 | −0.81 | 144 | 225.6 | 440.4 | 16.32: | 0.79 : | 0.60 : | | | | | | |
| 130 | 290.9 | 394.0 | 19.02 | 0.08 : | | 145 | 219.6 | 440.6 | 18.85 | −0.15 | | | | | | | |
| 131 | 330.7 | 402.2 | 16.39: | 1.76 :: | | 146 | 207.6 | 451.8 | 18.55: | 0.65 : | | | | | | | |
| 132 | 136.8 | 403.2 | 18.62 | 0.19 | | 147 | 101.6 | 454.8 | 17.70 | −0.04 | −0.30 | | | | | | |
| 133 | 42.5 | 403.3 | 18.11 | −0.12 | −0.39 | 148 | 169.9 | 463.9 | 17.82 | −0.11 | −0.64 | | | | | | |
| 134 | 152.3 | 405.1 | 18.54: | 1.52 : | | 149 | 120.7 | 479.0 | 18.89 | −0.18 | | | | | | | |
| 135 | 68.4 | 406.9 | 17.27: | 0.76 : | 0.34 :: | 150 | 112.9 | 480.6 | 18.73 | −0.05 | | | | | | | |

color–magnitude diagrams using the photometry collected by Rousseau *et al.* (1978). The magnitudes, colors, and spectral types from Rousseau *et al.* are presented in Table 9. The stars were dereddened for the color–magnitude diagrams and luminosity functions using the median reddening from the appropriate region. In Figs. 10 through 13, the three stars are plotted as asterisks.

We also note here that our field of view for LH 76 is slightly smaller than the area defined as LH 76 by Lucke (1972), and that the star SK-67 167, which has been classified by Conti *et al.* (1986) as O4f, is just off the chip. Another bright star in LH 76 which was too close to the edge for DAOPHOT, at coordinates of approximately $X=128$ and $Y=500$, is a star which was labeled as Galactic by Fehrenbach *et al.* (1965) by virtue of its radial velocity. [This is star number 17 in Fehrenbach *et al.* and star number 67 in Lucke (1972).]

### *3.3 LH 13*

LH 13 is one of the several OB associations comprising the emission region DEM 34 (Davies *et al.* 1976), or MC 18 as it is known at radio wavelengths (McGee *et al.* 1972). This extensive region of current star formation in the northwest corner of the LMC is second only to 30 Doradus in H$\alpha$ production in the LMC (Kennicutt & Hodge 1986). Comparison of the CO observations (Cohen *et al.* 1988) and the H$\alpha$ observations (Davies *et al.* 1976; Bothun 1990) show the region to be a "double blister," with stars forming at either end of a molecular cloud complex. Our optical image, which is a small subregion of this extensive star-forming complex, shows a tight cluster of stars in a region of heavy nebulosity, with a dust lane running through the center. This knot of nebulosity is NGC 1763. In Paper III, Parker *et al.* found the mass functions of LH 9 and LH 10, which are also in this star-forming complex, to be substantially different. They present a convincing case for sequential star formation, with LH 10 being triggered by the evolution of massive stars in LH 9.

In Fig. 10 we can see that the dereddened color–magnitude diagram for LH 13 shows a fairly clean main sequence down to about $V\approx 17$, which would be roughly $M_V\approx -1$, using a distance modulus to the LMC of 18.3 (in keeping with Paper I). This would correspond roughly to a B3 star on the Zero-Age Main Sequence (ZAMS) (Panagia 1973). However, there are a fair number of stars which are off the main sequence. For these stars, it is necessary to distinguish among foreground stars, evolved stars of the same age, an older background population, or stars which are part of the association but not coeval. The star shown as an asterisk, SK-66 41, has been classified by Rousseau *et al.* (1978) as Peculiar.

In Fig. 12 we have replotted the $V$ vs $B-V$ color–magnitude diagrams for the three associations, with the addition of the number of Galactic foreground stars expected from the model of Ratnatunga & Bahcall (1985). These numbers represent the average number of foreground stars expected in the indicated region of the dia-

TABLE 4. Photometry for stars in the region LH 76.

| Star | X | Y | V | B−V | U−B | Star | X | Y | V | B−V | U−B | Star | X | Y | V | B−V | U−B |
|---|---|---|---|---|---|---|---|---|---|---|---|---|---|---|---|---|---|
| 1 | 199.6 | 0.8 | 17.89:: | −0.42 :: | 0.00 :: | 41 | 110.0 | 109.8 | 17.48 | −0.12 | −0.94 | 81 | 262.1 | 160.6 | 15.81 | −0.14 | −1.12 |
| 2 | 51.4 | 2.0 | 16.62 | −0.13 | −0.47 | 42 | 208.1 | 112.1 | 15.26 | −0.19 | −1.10 | 82 | 118.3 | 163.4 | 17.04: | −0.19 : | −0.61 : |
| 3 | 7.0 | 6.6 | 17.85 | −0.19 | −0.56 | 43 | 69.8 | 112.3 | 18.80: | −0.15 : | −0.54 : | 83 | 166.5 | 164.4 | 16.86 | −0.15 | −0.90 |
| 4 | 54.4 | 17.2 | 18.71: | −0.11 : | −0.49 : | 44 | 234.7 | 114.1 | 18.31 | 0.00 | −0.70 | 84 | 195.5 | 166.8 | 18.16 | −0.22 | −0.60 |
| 5 | 74.5 | 25.2 | 17.58 | −0.05 | −0.77 | 45 | 37.8 | 116.6 | 17.91 | −0.03 | −0.38 | 85 | 183.3 | 166.9 | 17.76 | −0.20 | −0.67 |
| 6 | 177.1 | 28.7 | 18.99: | −0.14 : | −0.68 : | 46 | 161.3 | 117.6 | 17.91: | −0.27 | −0.40 | 86 | 120.6 | 170.5 | 13.88 | −0.20 | −0.96 :: |
| 7 | 149.9 | 30.3 | 13.35 | −0.20 :: | | 47 | 179.1 | 118.6 | 18.49: | −0.12 : | 0.01 :: | 87 | 112.6 | 171.1 | 16.55:: | −0.24 :: | −0.82 :: |
| 8 | 276.3 | 33.5 | 18.50 | 0.03 | −0.43 : | 48 | 49.4 | 119.2 | 18.23: | −0.07 : | −0.48 | 88 | 171.6 | 171.2 | 17.86 | −0.17 | −0.64 |
| 9 | 192.0 | 33.6 | 17.93 | 0.08 | −0.53 | 49 | 153.4 | 120.9 | 18.36:: | −0.40 : | −0.16 : | 89 | 50.3 | 171.4 | 15.95 | −0.18 | −0.92 |
| 10 | 5.0 | 37.1 | 17.81 | −0.08 | −0.56 | 50 | 3.7 | 123.5 | 18.53 | −0.16 | −0.62 | 90 | 142.5 | 172.2 | 17.84 | −0.05 | −0.74 |
| 11 | 120.2 | 39.9 | 18.14: | 0.62 : | −0.10 : | 51 | 87.4 | 124.0 | 15.59 | −0.17 | −0.98 | 91 | 21.8 | 172.4 | 17.88 | −0.06 | −0.79 |
| 12 | 58.9 | 44.4 | 16.83 | −0.14 | −0.77 | 52 | 66.4 | 125.1 | 17.00:: | −0.41 :: | −0.61 :: | 92 | 129.9 | 174.4 | 16.28 | −0.10 | −0.85 |
| 13 | 124.9 | 49.1 | 17.81 | −0.03 | −0.44 | 53 | 169.5 | 125.6 | 16.75: | −0.14 : | −0.84 : | 93 | 115.1 | 175.2 | 16.17:: | −0.12 :: | −1.03 :: |
| 14 | 147.4 | 51.3 | 17.39 | −0.09 | −0.83 | 54 | 163.1 | 126.8 | 18.70:: | 0.41 :: | −1.54 :: | 94 | 78.0 | 175.4 | 15.72 | −0.21 | −1.03 |
| 15 | 180.6 | 51.8 | 16.00 | −0.10 | −0.86 | 55 | 79.7 | 127.1 | 16.67:: | 0.11 :: | −0.66 :: | 95 | 122.2 | 180.0 | 17.87:: | −0.12 :: | −0.50 :: |
| 16 | 213.2 | 53.0 | 16.46 | −0.12 | −0.99 | 56 | 33.6 | 128.5 | 18.99: | 0.06 : | −0.82 : | 96 | 18.9 | 180.4 | 16.75 | −0.14 | −0.80 |
| 17 | 22.5 | 57.1 | 18.48 | 0.04 | −0.22 : | 57 | 106.3 | 132.8 | 15.42 | 0.04 | −1.00 | 97 | 199.7 | 180.8 | 17.43 | −0.03 | −0.87 |
| 18 | 281.4 | 58.1 | 18.18 | −0.13 | −0.57 | 58 | 271.7 | 133.7 | 17.33 | −0.06 | −0.83 | 98 | 87.7 | 180.9 | 14.99 | −0.24 | −1.09 |
| 19 | 71.2 | 61.5 | 17.64 | −0.08 | −0.73 | 59 | 229.3 | 133.9 | 17.30 | −0.12 | −0.90 | 99 | 209.8 | 181.1 | 18.15 | −0.02 : | −0.65 : |
| 20 | 19.8 | 66.2 | 16.43 | −0.16 | −0.88 | 60 | 174.8 | 134.8 | 13.66 | −0.24 | −1.10 :: | 100 | 158.4 | 182.8 | 18.48 | −0.04 | −0.60 |
| 21 | 116.3 | 67.5 | 18.02 | −0.03 | −0.27 | 61 | 199.0 | 134.9 | 15.38 | −0.17 | −1.08 | 101 | 211.5 | 184.9 | 17.77 | −0.15 | −0.74 |
| 22 | 123.1 | 68.8 | 18.13 | 0.02 | −0.48 | 62 | 57.2 | 135.2 | 16.41 | −0.19 | −0.91 | 102 | 70.9 | 187.8 | 19.00:: | −0.22 :: | −1.13 :: |
| 23 | 116.1 | 75.5 | 17.42 | −0.14 | −0.68 | 63 | 152.6 | 136.0 | 18.02 | −0.01 | −0.64 | 103 | 210.2 | 190.5 | 16.51 | −0.16 | −0.74 |
| 24 | 292.7 | 76.6 | 17.57 | 0.09 | −0.93 | 64 | 83.1 | 136.8 | 17.35:: | −0.09 :: | | 104 | 134.2 | 190.8 | 18.46 | −0.07 | −0.68 |
| 25 | 33.9 | 79.6 | 18.42 | −0.02 | −0.83 | 65 | 185.9 | 137.9 | 13.87 | −0.21 | −0.98 :: | 105 | 243.2 | 190.8 | 14.74: | 0.70 : | 0.58 :: |
| 26 | 7.6 | 80.1 | 16.20 | −0.14 | −0.95 | 66 | 76.1 | 140.2 | 15.49: | −0.24 :: | −0.94 :: | 106 | 241.8 | 193.8 | 16.99:: | −0.15 :: | −0.91 :: |
| 27 | 244.1 | 81.5 | 17.83 | −0.03 | −0.68 | 67 | 60.0 | 140.9 | 15.94 | −0.19 | −0.95 | 107 | 264.8 | 197.0 | 17.46 | −0.17 | 1.03 :: |
| 28 | 90.5 | 90.0 | 18.49: | −0.04 | −0.72 | 68 | 31.9 | 141.6 | 16.89 | −0.15 | −0.87 | 108 | 257.6 | 197.8 | 15.73 | −0.19 | −1.02 |
| 29 | 81.2 | 91.7 | 15.56 | −0.19 | −0.96 | 69 | 177.9 | 142.9 | 11.96 | −0.19 | −1.10 :: | 109 | 80.4 | 199.5 | 14.66 | −0.20 | −1.05 |
| 30 | 29.4 | 92.3 | 17.76 | −0.17 | −0.71 | 70 | 25.4 | 144.5 | 17.49 | 0.20 | −0.75 | 110 | 182.3 | 199.8 | 18.47 | 0.30 : | −0.85 : |
| 31 | 159.1 | 92.7 | 17.29 | −0.01 | −0.68 | 71 | 165.7 | 145.5 | 16.73:: | −0.58 :: | −0.85 | 111 | 235.0 | 200.2 | 18.27 | −0.30 | −0.57 |
| 32 | 52.5 | 97.9 | 18.50: | 0.01 : | −0.73 : | 72 | 213.7 | 147.7 | 16.82 | −0.22 | −0.89 | 112 | 214.5 | 203.3 | 14.04 | −0.03 | −1.11 |
| 33 | 72.2 | 100.1 | 18.45:: | −0.25 : | −0.58 : | 73 | 118.5 | 148.0 | 16.86 | −0.12 | −0.96 | 113 | 184.1 | 206.2 | 18.14 | −0.07 | −0.92 |
| 34 | 194.1 | 104.1 | 18.06 | 0.16 | −0.16 | 74 | 157.6 | 149.9 | 15.50 | −0.21 | −0.81 | 114 | 264.3 | 206.8 | 17.47: | −0.08 : | 0.29 :: |
| 35 | 258.9 | 105.3 | 17.24 | −0.08 | −0.90 | 75 | 19.2 | 152.5 | 16.53 | −0.14 | −0.83 | 115 | 176.1 | 209.3 | 15.17 | −0.20 | −1.11 |
| 36 | 288.6 | 106.3 | 17.77 | −0.06 | −0.62 | 76 | 168.0 | 154.4 | 17.36:: | −0.25 :: | −0.69 :: | 116 | 111.1 | 210.5 | 18.32 | 0.22 | −0.82 |
| 37 | 198.8 | 107.1 | 18.09 | 0.04 | −0.79 | 77 | 186.4 | 155.8 | 15.99: | −0.24 :: | −0.90 : | 117 | 256.8 | 210.7 | 16.70: | −0.09 : | −0.72 : |
| 38 | 42.4 | 108.2 | 18.00 | −0.13 | 0.39 : | 78 | 115.3 | 157.3 | 16.36 | −0.16 | −0.74 | 118 | 250.6 | 211.9 | 17.44:: | −0.27 :: | −0.65 :: |
| 39 | 56.5 | 108.8 | 16.07 | −0.17 | −0.91 | 79 | 169.6 | 159.6 | 17.17 | −0.20 | −0.82 | 119 | 248.0 | 215.0 | 16.39: | −0.24 :: | −0.75 :: |
| 40 | 32.3 | 109.1 | 17.85: | 0.39 : | −0.71 : | 80 | 68.2 | 159.8 | 14.29 | −0.23 | −1.08 | 120 | 120.5 | 215.6 | 18.32 | 0.07 | −0.89 |

TABLE 4. (continued)

| Star | X | Y | V | B−V | U−B | Star | X | Y | V | B−V | U−B | Star | X | Y | V | B−V | U−B |
|---|---|---|---|---|---|---|---|---|---|---|---|---|---|---|---|---|---|
| 121 | 256.1 | 217.4 | 16.18:: | −0.21 :: | −0.60 | 156 | 69.7 | 277.4 | 16.41 | −0.19 | −1.00 | 191 | 147.3 | 361.5 | 16.38 | −0.12 | −0.86 |
| 122 | 197.4 | 217.8 | 17.97 | 0.00 | −0.82 | 157 | 206.6 | 282.1 | 17.31 | −0.11 | −0.98 | 192 | 190.6 | 361.6 | 16.22 | −0.19 | −1.10 |
| 123 | 45.0 | 218.2 | 18.13 | −0.09 | −0.61 | 158 | 119.5 | 284.7 | 18.27 | −0.06 | −0.43 | 193 | 211.9 | 366.8 | 17.97 | 0.00 | −1.05 |
| 124 | 169.6 | 218.4 | 17.05 | −0.17 | −0.74 | 159 | 213.1 | 285.4 | 18.56: | 0.03 : | −0.76 : | 194 | 233.3 | 368.6 | 17.35 | −0.08 | −0.87 |
| 125 | 174.0 | 219.8 | 17.85 | −0.16 | −0.74 | 160 | 60.6 | 286.9 | 17.22 | −0.12 | −0.60 | 195 | 198.7 | 374.9 | 14.89 | −0.16 | −1.02 |
| 126 | 253.2 | 221.1 | 15.39:: | −0.18 :: | −1.06 | 161 | 311.5 | 288.5 | 17.58 | −0.12 | −0.92 | 196 | 65.5 | 375.6 | 17.99 | 0.04 | −0.71 |
| 127 | 303.8 | 226.5 | 17.01 | −0.10 | −0.82 | 162 | 282.0 | 291.0 | 14.43 | −0.17 | −1.11 | 197 | 114.5 | 376.2 | 18.41 | 0.02 | −0.77 |
| 128 | 185.2 | 226.7 | 17.70 | −0.16 | −0.55 | 163 | 134.9 | 296.9 | 17.60 | −0.04 | −0.89 | 198 | 82.3 | 377.4 | 16.50 | −0.15 | −0.85 |
| 129 | 180.5 | 227.2 | 15.39 | −0.22 | −1.02 | 164 | 142.1 | 306.4 | 15.37 | −0.17 | −0.93 | 199 | 168.6 | 377.4 | 17.04 | −0.11 | −0.92 |
| 130 | 244.7 | 229.9 | 15.99 | −0.19 | −0.95 | 165 | 91.0 | 307.9 | 18.72: | 0.14 : | −0.76 : | 200 | 161.2 | 383.0 | 17.01 | −0.08 | −0.61 |
| 131 | 155.5 | 232.0 | 16.88 | −0.20 | −0.87 | 166 | 224.9 | 308.0 | 16.80 | 0.12 : | −1.01 : | 201 | 18.4 | 383.6 | 17.04 | −0.14 | −0.88 |
| 132 | 106.2 | 232.3 | 17.10 | 0.03 | −0.52 | 167 | 54.0 | 311.1 | 18.01 | −0.08 | −0.62 | 202 | 86.8 | 384.3 | 17.59 | −0.11 | −0.66 |
| 133 | 143.8 | 235.7 | 16.65 | −0.16 | −0.89 | 168 | 245.7 | 313.9 | 17.17:: | −0.17 : | −0.34 : | 203 | 259.3 | 385.4 | 16.56 | −0.04 | −0.86 |
| 134 | 153.0 | 236.5 | 17.53 | −0.09 | −0.63 | 169 | 221.1 | 314.6 | 15.23:: | −0.23 :: | −0.96 :: | 204 | 96.8 | 386.5 | 18.29:: | 0.03 :: | −0.47 :: |
| 135 | 255.2 | 237.6 | 18.26: | −0.22 : | −1.05 :: | 170 | 114.8 | 314.8 | 17.13 | −0.14 | −0.77 | 205 | 152.8 | 396.3 | 17.42 | 0.14 | −0.75 |
| 136 | 170.1 | 239.7 | 11.91 | −0.22 | −1.14 | 171 | 295.2 | 315.8 | 18.77: | −0.14 : | −0.43 : | 206 | 91.5 | 406.7 | 18.43 | 0.03 | −0.90 |
| 137 | 186.9 | 240.8 | 17.74 | −0.30 | −0.61 | 172 | 108.9 | 318.4 | 16.44 | −0.14 | −0.88 | 207 | 195.6 | 409.3 | 19.14: | −0.16 : | −0.58 :: |
| 138 | 245.6 | 241.7 | 16.42 | −0.18 | −0.88 | 173 | 158.8 | 320.3 | 17.33 | −0.14 | −0.73 | 208 | 21.1 | 412.4 | 17.81 | −0.09 | −0.45 |
| 139 | 203.4 | 242.6 | 17.02 | −0.12 | −0.86 | 174 | 184.3 | 325.6 | 17.34:: | 0.19 :: | −1.29 :: | 209 | 95.0 | 420.3 | 18.48: | −0.06 | −0.50 |
| 140 | 133.3 | 245.3 | 18.79 | 0.08 : | −0.66 : | 175 | 173.6 | 327.4 | 12.31 | −0.21 :: | −1.02 :: | 210 | 67.4 | 424.8 | 18.27 | 0.34 | −1.11 : |
| 141 | 171.8 | 250.0 | 15.29: | −0.10 : | −1.05 : | 176 | 79.3 | 331.7 | 13.46 | −0.14 | −1.03 | 211 | 294.7 | 425.0 | 14.14:: | 0.03 :: | −0.93 |
| 142 | 167.5 | 252.7 | 13.96 | −0.26 | −1.08 | 177 | 275.1 | 333.9 | 18.18 | 0.00 | −0.56 | 212 | 42.9 | 425.7 | 18.48 | 0.19 | −0.54 : |
| 143 | 262.9 | 253.3 | 18.29 | 0.23 | −1.14 | 178 | 185.1 | 334.2 | 15.93: | −0.29 : | −0.93 | 213 | 67.6 | 433.7 | 15.24 | −0.18 | −1.03 |
| 144 | 35.1 | 254.5 | 18.27 | −0.19 | −0.63 | 179 | 122.8 | 334.3 | 17.80 | 0.06 | −0.62 | 214 | 289.5 | 434.7 | 17.10 | −0.16 | −0.14 |
| 145 | 134.4 | 258.0 | 18.94: | 0.16 : | −0.94 : | 180 | 206.5 | 335.7 | 16.30: | −0.21 : | −1.01 | 215 | 60.8 | 435.9 | 15.76 | −0.18 | −1.00 |
| 146 | 12.6 | 258.6 | 19.02: | 0.14 : | −0.65 :: | 181 | 151.8 | 336.9 | 18.67:: | −0.06 :: | −0.61 :: | 216 | 206.3 | 441.1 | 15.93 | −0.14 | −0.67 |
| 147 | 63.3 | 260.9 | 14.31 | −0.19 | −1.07 | 182 | 24.3 | 341.1 | 18.34 | −0.03 | −0.48 | 217 | 26.3 | 447.8 | 18.12 | 0.06 | −0.65 |
| 148 | 287.4 | 261.2 | 18.06: | 0.71 : | −0.44 : | 183 | 15.7 | 343.9 | 17.81 | −0.03 | −0.61 | 218 | 11.3 | 456.3 | 18.75: | 0.22 : | −0.61 :: |
| 149 | 82.0 | 263.7 | 18.90: | 0.01 : | −0.80 : | 184 | 207.5 | 344.5 | 18.09: | 0.16 : | −0.47 :: | 219 | 251.3 | 465.3 | 18.07 | −0.07 | −0.69 |
| 150 | 216.7 | 264.7 | 17.57 | 0.01 | −1.00 | 185 | 162.3 | 349.3 | 14.93 | −0.21 | −0.98 | 220 | 100.3 | 484.6 | 15.41 | 0.07 | −0.87 |
| 151 | 18.8 | 267.1 | 18.78 | −0.03 : | −0.32 : | 186 | 110.9 | 349.5 | 13.13 | −0.19 | −0.97 | 221 | 282.9 | 489.9 | 18.10 | 0.06 | −0.60 |
| 152 | 189.9 | 268.2 | 14.12 | −0.18 | −1.13 | 187 | 271.9 | 352.0 | 16.81 | −0.13 | −0.97 | 222 | 51.5 | 496.2 | 17.73 | 0.01 | −0.90 |
| 153 | 235.1 | 268.3 | 16.03 | −0.06 | −0.91 | 188 | 170.0 | 352.1 | 18.28: | 0.19 : | −1.34 | | | | | | |
| 154 | 57.8 | 269.6 | 17.61 | −0.29 | −0.46 | 189 | 193.0 | 352.2 | 18.23: | 0.10 : | −0.68 : | | | | | | |
| 155 | 133.2 | 274.4 | 17.04 | −0.07 | −0.76 | 190 | 89.7 | 360.7 | 14.22 | −0.21 | −1.11 | | | | | | |

TABLE 5. Photometry for stars in the northern region of LH 105.

| Star | X | Y | V | B−V | U−B | Star | X | Y | V | B−V | U−B | Star | X | Y | V | B−V | U−B |
|---|---|---|---|---|---|---|---|---|---|---|---|---|---|---|---|---|---|
| 1 | 18.3 | 24.9 | 17.31: | 1.56 : | | 42 | 232.1 | 246.1 | 17.70: | 0.62 : | | 83 | 192.1 | 337.2 | 15.67 | 0.45 | −0.58 |
| 2 | 42.2 | 27.5 | 17.99: | 1.21 : | | 43 | 215.6 | 246.6 | 16.56 | 0.25 | −0.38 | 84 | 185.0 | 337.9 | 16.45: | 1.98 :: | |
| 3 | 203.6 | 34.5 | 17.25 | 0.38 | −0.62 | 44 | 94.1 | 248.6 | 15.57 | −0.01 | −0.67 | 85 | 127.0 | 338.4 | 16.59 | 0.16 | −0.57 |
| 4 | 144.2 | 36.8 | 18.01: | 0.56 : | | 45 | 291.4 | 249.9 | 17.35 | 0.04 | −0.07 | 86 | 267.5 | 338.4 | 17.61 | 0.47 | |
| 5 | 85.8 | 72.5 | 16.41 | 0.08 | −0.72 | 46 | 207.7 | 250.0 | 16.78: | 0.59 : | −0.58 : | 87 | 114.6 | 338.6 | 12.53:: | −0.11 :: | −0.96 :: |
| 6 | 31.8 | 72.8 | 16.79: | 0.91 : | −0.85 : | 47 | 118.3 | 251.6 | 16.43 | 0.34 | −0.60 | 88 | 89.9 | 340.8 | 15.37 | 0.13 | −0.78 |
| 7 | 77.5 | 77.5 | 17.08 | 0.00 | −0.76 | 48 | 76.5 | 252.6 | 18.32 | 0.25 | | 89 | 102.1 | 344.4 | 14.63 | −0.10 | −0.91 |
| 8 | 61.5 | 80.0 | 16.09: | 0.87 : | 0.84 : | 49 | 48.3 | 254.2 | 17.24 | 0.30 | −0.66 | 90 | 20.9 | 347.9 | 17.87 | 0.19 | |
| 9 | 151.6 | 87.7 | 17.80 | −0.06 | −0.61 | 50 | 151.7 | 257.9 | 14.67 | 0.14 | −0.77 | 91 | 198.6 | 347.9 | 18.22 | −0.08 | |
| 10 | 289.7 | 91.3 | 18.03 | 0.10 | −0.71 | 51 | 270.5 | 260.2 | 16.96 | 0.41 | −0.51 | 92 | 81.8 | 359.2 | 17.71 | 0.03 | −0.34 |
| 11 | 129.7 | 94.7 | 16.39 | 0.00 | −0.63 | 52 | 190.4 | 261.5 | 17.37 | 0.40 | −0.56 | 93 | 182.2 | 361.6 | 18.08: | 0.51 : | |
| 12 | 159.4 | 107.9 | 16.92 | 0.20 | −0.76 | 53 | 70.9 | 261.7 | 18.46: | 2.00 :: | | 94 | 208.7 | 366.6 | 18.25 | −0.34 | −0.43 |
| 13 | 222.3 | 109.7 | 16.73: | 1.86 : | | 54 | 249.9 | 262.0 | 16.57 | 0.23 | −0.66 | 95 | 79.1 | 370.5 | 16.43: | 2.13 :: | |
| 14 | 76.4 | 109.8 | 14.65 | 0.09 | −0.96 | 55 | 295.7 | 263.1 | 16.11: | 0.85 : | 0.18 : | 96 | 186.5 | 370.8 | 17.55 | 0.28 | −0.56 |
| 15 | 138.2 | 120.7 | 17.44 | 0.02 | −0.35 | 56 | 274.2 | 265.5 | 16.28 | 0.41 | −0.44 | 97 | 137.2 | 373.9 | 16.20 | −0.01 | −0.91 |
| 16 | 93.1 | 125.5 | 17.64 | −0.05 | −0.73 | 57 | 269.6 | 269.8 | 16.17: | 0.56 : | −0.50 : | 98 | 192.5 | 376.6 | 17.69 | −0.17 | |
| 17 | 178.8 | 127.8 | 14.68 | 0.31 | −0.82 | 58 | 102.7 | 271.8 | 17.39 | 0.04 | −0.64 | 99 | 201.6 | 377.4 | 16.50 | 0.40 | −0.47 |
| 18 | 116.9 | 132.1 | 15.96 | −0.01 | −0.74 | 59 | 96.6 | 271.9 | 17.74 | −0.07 | −0.21 | 100 | 186.8 | 380.0 | 17.45: | 0.20 | −0.68 |
| 19 | 173.1 | 134.3 | 16.43:: | 0.30 :: | −1.06 : | 60 | 263.9 | 274.5 | 14.98 | 0.47 | −0.63 | 101 | 90.5 | 384.4 | 17.25 | −0.05 | −0.80 |
| 20 | 190.5 | 139.4 | 16.66 | 0.49 | −0.48 | 61 | 117.5 | 274.7 | 16.12 | 0.07 | −0.70 | 102 | 208.3 | 390.3 | 17.26: | 0.81 : | |
| 21 | 90.2 | 140.3 | 13.90: | 0.76 : | 0.86 : | 62 | 265.6 | 277.7 | 15.71 | 0.38 | −0.73 | 103 | 294.6 | 392.6 | 16.23 | 0.07 | −0.56 |
| 22 | 174.9 | 140.9 | 12.10:: | 0.34 :: | −0.58 :: | 63 | 95.1 | 281.3 | 17.31 | 0.09 | 0.38 | 104 | 89.8 | 395.1 | 14.23 | −0.11 | −0.93 |
| 23 | 219.6 | 143.3 | 17.90 | 0.14 | −0.68 | 64 | 124.1 | 283.2 | 17.57 | 0.10 | −0.55 | 105 | 288.0 | 403.3 | 16.08 | 0.10 | −0.59 |
| 24 | 64.8 | 145.5 | 17.57 | 0.24 | −0.64 | 65 | 27.0 | 283.6 | 15.78 | 0.07 | −0.74 | 106 | 94.0 | 405.0 | 17.79 | −0.17 | |
| 25 | 78.8 | 149.6 | 17.65: | 0.75 : | | 66 | 20.6 | 284.0 | 16.26 | 0.00 | −0.45 | 107 | 277.6 | 406.9 | 16.91 | 0.06 | −0.51 |
| 26 | 293.5 | 150.1 | 17.96 | −0.05 | | 67 | 301.5 | 284.1 | 16.34: | 0.89 : | −0.11 : | 108 | 233.3 | 411.6 | 15.65: | 0.68 : | −0.36 : |
| 27 | 158.0 | 155.9 | 17.32 | −0.01 | −0.59 | 68 | 79.6 | 286.2 | 17.91: | 0.58 : | | 109 | 239.8 | 413.6 | 16.19: | 0.60 : | −0.81 : |
| 28 | 148.9 | 157.3 | 14.94 | −0.04 | −0.89 | 69 | 13.6 | 291.5 | 18.02 | −0.08 | −0.42 | 110 | 157.9 | 413.7 | 15.65 | −0.06 | −0.82 |
| 29 | 285.8 | 164.5 | 15.21: | 1.46 : | 0.88 : | 70 | 159.3 | 298.9 | 14.26 | 0.04 | −0.86 | 111 | 49.5 | 414.9 | 18.16 | 0.10 | |
| 30 | 133.7 | 167.0 | 17.19 | 0.10 | −0.46 | 71 | 148.3 | 300.5 | 17.90 | 0.08 | | 112 | 242.3 | 414.9 | 16.43 | 0.38 | −0.41 |
| 31 | 185.7 | 172.8 | 16.59 | 0.39 | −0.44 | 72 | 108.4 | 306.2 | 16.87 | −0.05 | −0.62 | 113 | 234.3 | 420.2 | 16.91: | 1.40 : | |
| 32 | 47.3 | 182.6 | 18.03 | −0.40 | | 73 | 63.3 | 309.0 | 17.56 | −0.06 | −0.14 | 114 | 266.0 | 422.4 | 17.68: | 0.59 : | −0.52 : |
| 33 | 149.3 | 191.8 | 18.40 | −0.05 | −0.94 | 74 | 235.4 | 316.5 | 17.18 | −0.01 | −0.80 | 115 | 153.2 | 423.4 | 16.93: | 1.41 : | |
| 34 | 210.2 | 194.4 | 16.52 | 0.28 | −0.69 | 75 | 99.0 | 320.3 | 17.52 | 0.05 | −0.92 | 116 | 33.2 | 426.5 | 16.42: | 1.38 : | |
| 35 | 296.8 | 195.4 | 16.29 | 0.35 | −0.56 | 76 | 41.0 | 325.7 | 16.56 | 0.03 | −0.86 | 117 | 282.9 | 431.8 | 15.55 | 0.22 | −0.59 |
| 36 | 133.3 | 197.8 | 17.87 | −0.03 | −0.50 | 77 | 137.6 | 327.9 | 18.17 | 0.25 | | 118 | 211.5 | 443.8 | 16.77: | 1.62 : | |
| 37 | 100.6 | 204.8 | 14.32 | −0.10 | −0.97 | 78 | 219.6 | 327.9 | 16.47: | 0.57 : | −0.72 : | 119 | 218.7 | 444.2 | 18.14 | −0.13 | |
| 38 | 204.7 | 214.9 | 16.83: | 1.58 : | | 79 | 298.2 | 328.5 | 16.82 | 0.09 | −0.40 | 120 | 293.4 | 446.5 | 15.82:: | 0.17 :: | −0.77 : |
| 39 | 59.3 | 229.5 | 15.97: | 0.86 : | 1.03 :: | 80 | 81.6 | 328.8 | 17.22: | 1.24 : | | 121 | 50.3 | 459.5 | 17.23 | −0.08 | −0.51 |
| 40 | 280.0 | 241.1 | 15.13: | 0.59 : | 0.02 : | 81 | 197.5 | 329.0 | 17.46: | 0.56 : | | 122 | 88.6 | 496.1 | 14.44: | 1.27 : | 2.13 :: |
| 41 | 163.7 | 243.3 | 15.82 | 0.16 | −0.87 | 82 | 38.5 | 333.3 | 16.80: | 1.55 : | | 123 | 202.6 | 497.0 | 16.65: | 0.77 : | −0.28 : |

TABLE 6. Photometry for stars in the southern region of LH 105.

| Star | X | Y | V | B−V | U−B | Star | X | Y | V | B−V | U−B | Star | X | Y | V | B−V | U−B |
|---|---|---|---|---|---|---|---|---|---|---|---|---|---|---|---|---|---|
| 1 | 216.8 | 15.7 | 16.35 | 0.18 | −0.52 | 36 | 40.5 | 208.7 | 18.46 | −0.18 | | 71 | 194.7 | 347.9 | 14.93:: | 0.11 :: | −0.74 |
| 2 | 81.2 | 43.1 | 18.13: | 1.32 : | | 37 | 34.8 | 210.5 | 16.18 | 0.19 | −0.69 | 72 | 55.8 | 348.4 | 13.99 | 0.12 | −0.72 |
| 3 | 129.9 | 49.0 | 17.15 | 0.21 | −0.55 | 38 | 17.3 | 211.1 | 18.00 | 0.17 | −0.17 | 73 | 47.2 | 356.4 | 16.82 | 0.22 | −0.58 |
| 4 | 50.4 | 52.0 | 17.36: | 2.33 :: | | 39 | 259.2 | 221.1 | 17.27: | 1.13 : | | 74 | 163.7 | 356.8 | 16.76: | 2.05 : | |
| 5 | 71.5 | 56.3 | 18.05: | 0.67 : | | 40 | 138.1 | 223.2 | 17.86 | −0.23 | 0.34 | 75 | 169.8 | 358.0 | 17.67 | 0.09 | −0.58 |
| 6 | 203.1 | 61.6 | 17.03 | 0.05 | −0.77 | 41 | 129.1 | 226.0 | 18.60 | −0.60 | | 76 | 121.5 | 363.6 | 17.05: | 2.07 : | |
| 7 | 220.7 | 73.3 | 17.97 | 0.08 | | 42 | 22.2 | 232.4 | 17.15 | 0.16 | −0.64 | 77 | 242.1 | 365.0 | 17.87: | 1.23 : | |
| 8 | 296.7 | 78.9 | 16.00: | 0.94 : | 0.38 :: | 43 | 226.8 | 235.0 | 18.36: | 0.61 : | | 78 | 291.8 | 368.8 | 17.90 | −0.01 | 1.04 :: |
| 9 | 53.6 | 83.8 | 17.85 | 0.05 | −1.10 | 44 | 296.1 | 240.0 | 17.19: | 0.92 : | | 79 | 71.8 | 376.6 | 17.66 | 0.10 | |
| 10 | 54.4 | 83.9 | 17.41 | 0.46 | | 45 | 25.6 | 243.8 | 18.01 | 0.28 | | 80 | 3.6 | 389.8 | 16.04 | 0.14 | −0.73 |
| 11 | 38.5 | 90.6 | 16.15: | 0.51 : | −0.41 : | 46 | 24.0 | 260.0 | 14.43 | 0.30 | −0.57 | 81 | 16.1 | 393.7 | 15.55 | 0.25 | −0.69 |
| 12 | 184.3 | 100.8 | 18.36: | 1.07 : | | 47 | 65.8 | 276.3 | 17.02: | 1.42 : | | 82 | 62.2 | 396.5 | 15.30 | 0.23 | −0.54 |
| 13 | 197.4 | 101.1 | 16.61 | 0.12 | −0.42 | 48 | 11.1 | 276.4 | 17.77: | 1.68 : | | 83 | 7.6 | 403.7 | 16.72 | 0.29 | −0.74 |
| 14 | 20.0 | 103.7 | 16.83 | 0.44 | −0.58 | 49 | 60.3 | 276.8 | 16.05 | 0.15 | −0.44 | 84 | 21.1 | 407.3 | 17.74: | 1.46 : | −2.67 : |
| 15 | 297.2 | 109.0 | 16.28: | 0.56 : | 0.62 : | 50 | 29.0 | 285.9 | 18.04 | 0.22 | | 85 | 16.0 | 409.6 | 13.87:: | 0.10 :: | −0.65 |
| 16 | 27.9 | 113.7 | 18.81: | 0.89 :: | | 51 | 12.9 | 289.1 | 16.47: | 0.85 : | | 86 | 39.8 | 410.3 | 17.35 | 0.16 | −0.29 |
| 17 | 102.0 | 114.2 | 16.65 | 0.10 | −0.39 | 52 | 116.3 | 289.3 | 18.46 | 0.40 | | 87 | 135.5 | 415.1 | 16.87: | 1.35 : | |
| 18 | 150.1 | 115.0 | 17.91 | 0.15 | −0.95 | 53 | 306.9 | 294.6 | 17.93 | 0.31 | | 88 | 3.8 | 415.9 | 16.99: | 1.68 : | |
| 19 | 54.3 | 115.3 | 15.69 | 0.05 | −0.57 | 54 | 88.8 | 295.2 | 16.60: | 1.86 : | | 89 | 70.2 | 419.7 | 17.85: | 0.82 : | |
| 20 | 159.3 | 120.8 | 15.35 | 0.12 | −0.54 | 55 | 239.4 | 295.9 | 17.80 | −0.08 | −0.31 | 90 | 155.2 | 427.0 | 16.81: | 1.74 : | |
| 21 | 91.2 | 126.0 | 14.90 | −0.07 | −0.78 :: | 56 | 100.7 | 297.7 | 18.03: | 1.43 : | | 91 | 45.5 | 428.7 | 18.24 | −0.03 | |
| 22 | 89.8 | 127.2 | 14.51:: | 0.15 | −0.72 : | 57 | 43.7 | 305.3 | 18.45: | 0.40 : | | 92 | 224.2 | 432.8 | 16.44: | 1.19 : | |
| 23 | 115.1 | 128.8 | 16.82: | 0.51 : | −0.65 : | 58 | 104.4 | 305.4 | 18.45: | 0.86 : | | 93 | 173.4 | 433.0 | 15.85 | −0.11 | −0.90 |
| 24 | 80.1 | 129.4 | 16.71 | 0.10 | −0.75 | 59 | 94.6 | 306.1 | 18.05 | −0.25 | | 94 | 127.9 | 440.3 | 16.98: | 2.06 : | |
| 25 | 103.0 | 132.2 | 17.83 | 0.33 | | 60 | 98.8 | 309.7 | 18.02: | 0.64 : | | 95 | 21.0 | 443.7 | 17.79 | 0.00 | |
| 26 | 82.5 | 138.5 | 17.44: | 0.42 : | | 61 | 57.2 | 315.4 | 16.69 | 0.31 | −0.14 | 96 | 189.7 | 465.0 | 16.53: | 0.69 : | |
| 27 | 78.4 | 148.1 | 16.03 | 0.11 | −0.40 | 62 | 154.8 | 338.8 | 15.90 | 0.08 | −0.65 | 97 | 177.7 | 468.7 | 18.59: | 1.18 :: | |
| 28 | 175.0 | 149.3 | 16.84: | 1.64 : | | 63 | 281.5 | 340.7 | 17.22 | −0.23 | −0.63 | 98 | 61.8 | 469.0 | 18.60: | −0.08 | |
| 29 | 165.2 | 152.0 | 16.72: | 1.77 : | | 64 | 241.9 | 342.2 | 17.62: | 0.56 : | | 99 | 222.1 | 473.5 | 18.05: | 1.08 : | |
| 30 | 98.0 | 156.1 | 16.51: | 0.51 : | −0.76 : | 65 | 62.0 | 342.4 | 17.22: | 2.01 : | | 100 | 117.1 | 475.5 | 16.50: | 1.65 : | |
| 31 | 203.1 | 177.0 | 17.90 | 0.01 | | 66 | 249.8 | 343.6 | 18.63: | −0.06 : | | 101 | 58.3 | 478.8 | 17.41: | 1.13 : | |
| 32 | 25.8 | 185.2 | 17.98 | −0.02 | −0.40 | 67 | 197.3 | 344.5 | 15.99:: | 0.19 :: | −0.60 : | | | | | | |
| 33 | 229.0 | 191.5 | 16.05: | 0.59 : | 0.36 : | 68 | 81.2 | 344.7 | 16.41 | 0.34 | −0.70 | | | | | | |
| 34 | 315.4 | 193.4 | 17.91 | 0.42 | | 69 | 145.8 | 345.9 | 15.24 | 0.06 | −0.74 | | | | | | |
| 35 | 113.4 | 198.3 | 17.61: | 1.69 : | | 70 | 292.4 | 346.0 | 15.49: | 1.34 : | | | | | | | |

TABLE 7. Star cross identifications.

| Star | $\alpha_{2000}$ | $\delta_{2000}$ | Other Designations[1] |
|---|---|---|---|
| | | LH 13 | |
| 62 | 04 57 40.62 | -66 27 24.9 | G 8889 522 |
| 97 | 04 57 45.18 | -66 27 54.1 | G 8889 537 |
| | | LH 76 | |
| 7 | 05 32 01.74 | -67 41 01.8 | L 53 |
| 15 | 03.57 | 41 16.9 | L 54 |
| 39 | 08.64 | 40 15.9 | L 52 |
| 42 | 08.76 | 41 30.3 | L 56 |
| 57 | 10.66 | 40 40.3 | L 55 |
| 69 | 11.45 | 41 15.5 | Sk -67 174, G 9162 478 |
| 80 | 13.03 | 40 21.6 | L 49 |
| 81 | 12.90 | 41 56.7 | L 64 |
| 86 | 13.90 | 40 47.3 | G 9162 62 |
| 89 | 14.06 | 40 12.8 | L 50 |
| 109 | 16.45 | 40 27.5 | L 48 |
| 136 | 19.84 | 41 11.5 | Sk -67 176, G 9162 100 |
| 147 | 21.78 | 40 19.0 | L 47 |
| 162 | 24.17 | 42 06.3 | L 62 |
| 164 | 25.64 | 40 57.6 | L 58 |
| 175 | 27.43 | 41 13.0 | Sk -67 178b, G 9162 144 |
| 176 | 27.88 | 40 26.7 | L 46 |
| 185 | 29.33 | 41 07.4 | L 60 |
| 186 | 29.39 | 40 42.2 | L 44 |
| 195 | 31.51 | 41 25.2 | L 61 |
| | | LH 105 North | |
| 22 | 05 39 41 | -69 44[2] | R 148, Sk -69 254, DD 1 |
| 87 | 05 39 59 | -69 44[2] | R 149, Sk -69 257, DD 3 |
| 5 | – | – | CCH 34 |
| 14 | – | – | CCH 21 |
| 17 | – | – | CCH 32 |
| 18 | – | – | CCH 23 |
| 21 | – | – | CCH 22 |
| 37 | – | – | DD 8 |
| 44 | – | – | CCH 24 |
| 50 | – | – | DD 9 |
| 70 | – | – | DD 10 |
| 88 | – | – | CCH 26 |
| 89 | – | – | CCH 27 |
| 104 | – | – | DD 11 |
| | | LH 105 South | |
| 21 | – | – | DD 13 |
| 46 | – | – | CCH 33 |

Notes to TABLE 7

[1]G, HST Guide Star Catalog (1992); L, Lucke (1972); Sk, Sanduleak (1969); DD, Dufour and Duval (1975); CCH, Cowley et al. (1978); R, Feast et al. (1960).

[2]Approximate coordinates from Sanduleak (1969).

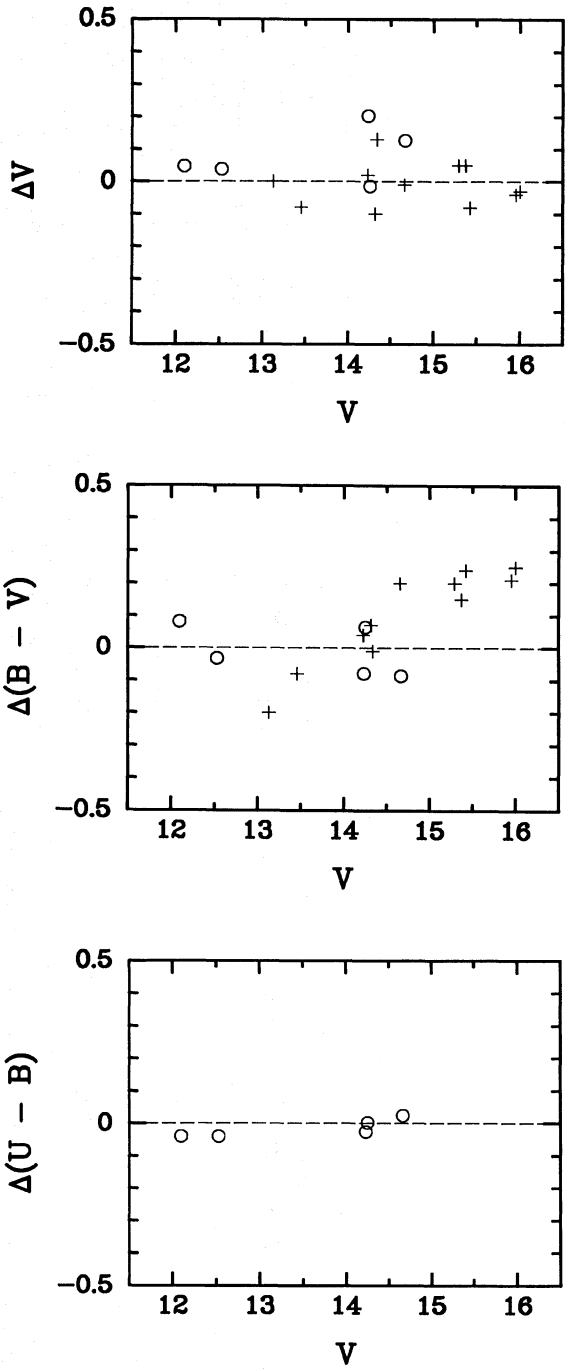


FIG. 8. A comparison of the photometry presented here with that of Lucke (1972) and Dufour & Duval (1975) for the stars in common. The sense of the difference is our magnitude minus theirs, which is plotted against $V$ magnitude. The crosses represent Lucke's photographic iris photometry, and the circles represent the photoelectric photometry of Dufour and Duval.

grams for the angular area of the CCD frame(s) for each association. While these numbers should not be overinterpreted, they provide a useful tool for understanding the diagrams. For LH 13 we see that the stars with $0.8 < B-V < 1.3$ are in fact reasonably likely to be foreground stars, as is the star at $V \approx 17.5$ and $B-V \approx 1.5$. However, the very

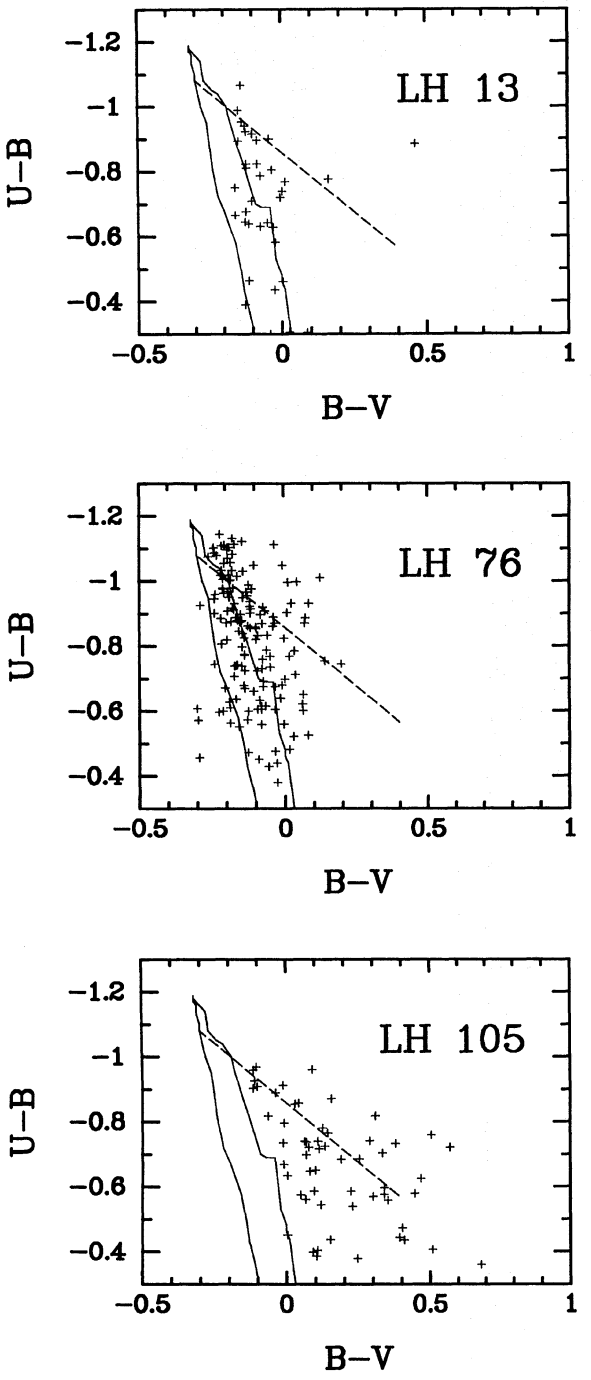


FIG. 9. Two-color relation for stars in the three observed regions. The solid lines show the intrinsic colors for main-sequence and supergiant stars given by Fitzgerald (1970). The dashed line represents the reddening vector for an O9.5 star. Only stars with "good" photometry, as defined in the text, are shown.

red star at $V \approx 13.5$ is in fact likely to be a red supergiant, and will need a spectrum to determine its true nature. The stars with $0.2 < B-V < 0.8$ appear to belong to some older population of stars. Examination of the spatial distribution of the stars shows them to be coincident with the main stars in the cluster, and thus at least good candidates for stars created in a noncoeval event. When all the stars are properly placed on a theoretical H-R diagram, we should be able to discern their true nature.

TABLE 8. Derived color excesses.

| Region | Median | Mean | $\sigma$ | Number of stars used |
|---|---|---|---|---|
| LH 13 | 0.16 | 0.19 | 0.14 | 37 |
| LH 76 | 0.13 | 0.16 | 0.10 | 147 |
| LH 105 | 0.38 | 0.45 | 0.21 | 58 |

### *3.4 LH 76*

LH 76 is one of several star-forming regions in the southern edge of Constellation III, a ring of current star formation which surrounds a hole in the interstellar medium blown out by a relatively recent episode of star formation. Constellation III is in the northeast of the LMC. The association LH 76 is also called NGC 2014, and its H II region is DEM 229 (Davies *et al.* 1976).

In examining the color–magnitude diagrams for LH 76 in Figs. 11 and 12, we find no evidence for contamination by an older population. In Fig. 10 the star on the main sequence plotted as an asterisk, SK-67 173, was classified by Sanduleak (1969) as OB. The star with $V \approx 9.5$ and $B-V \approx 1$ is SK-67 178a, which was classified by Rousseau *et al.* (1978) as G2Ia. In Fig. 12, we can see that all the other stars off the main sequence (with the exception of SK-67 178a) are very likely to be foreground stars. With only one supergiant, the region is almost certainly coeval. It seems likely that the star formation was triggered by the winds which blew out the hole which is the center of Constellation III.

### *3.5 LH 105*

The OB association LH 105 lies at the southern edge of the greater region of star formation centered around 30 Doradus. The knot of nebulosity in the southern region is NGC 2079; the wispy H II region surrounding the entire association is DEM 271 (Davies *et al.* 1976). LH 105's only claim to fame is the x-ray source LMC X-1, which is a candidate for a black hole and an x-ray ionized nebula (see Pakull & Angebault 1987, and references within.) Inspection of the finding chart in Pakull and Angebault (1987) shows that their candidate, star "32," is probably our star number 17 in the northern region. They give a spectral type of O7 for this star, and suggest that it is the optical counterpart to the x-ray source.

The reddening is quite high in LH 105, with a median $E(B-V)$ of 0.38 and a mean of 0.45. Inspection of the color–color diagram in Fig. 9 shows that the spread in reddening is as much as 0.5 mag. Using the median reddening is probably a little too much for LH 105; in Fig. 10, it is apparent that the faintest main-sequence stars have been shifted a little too much to the blue. We checked the

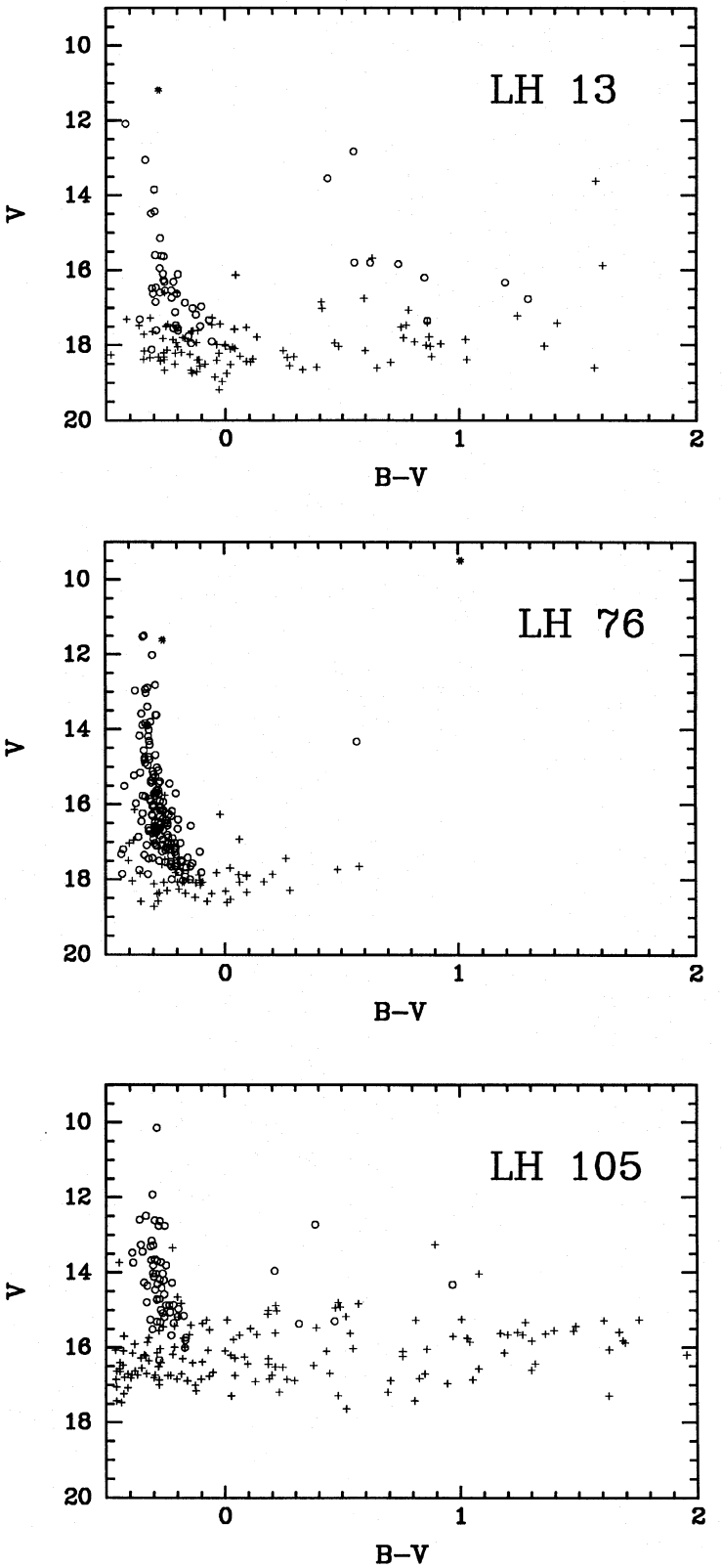


FIG. 10. Dereddened color–magnitude diagrams in $V$ vs $B-V$ for the three regions. Stars with "good" photometry, i.e., those stars with uncertainties in magnitudes and colors less than 0.07 mag, are represented by circles. The remaining stars are represented by crosses. The stars marked as asterisks were unresolved by DAOPHOT, and are taken from the literature.

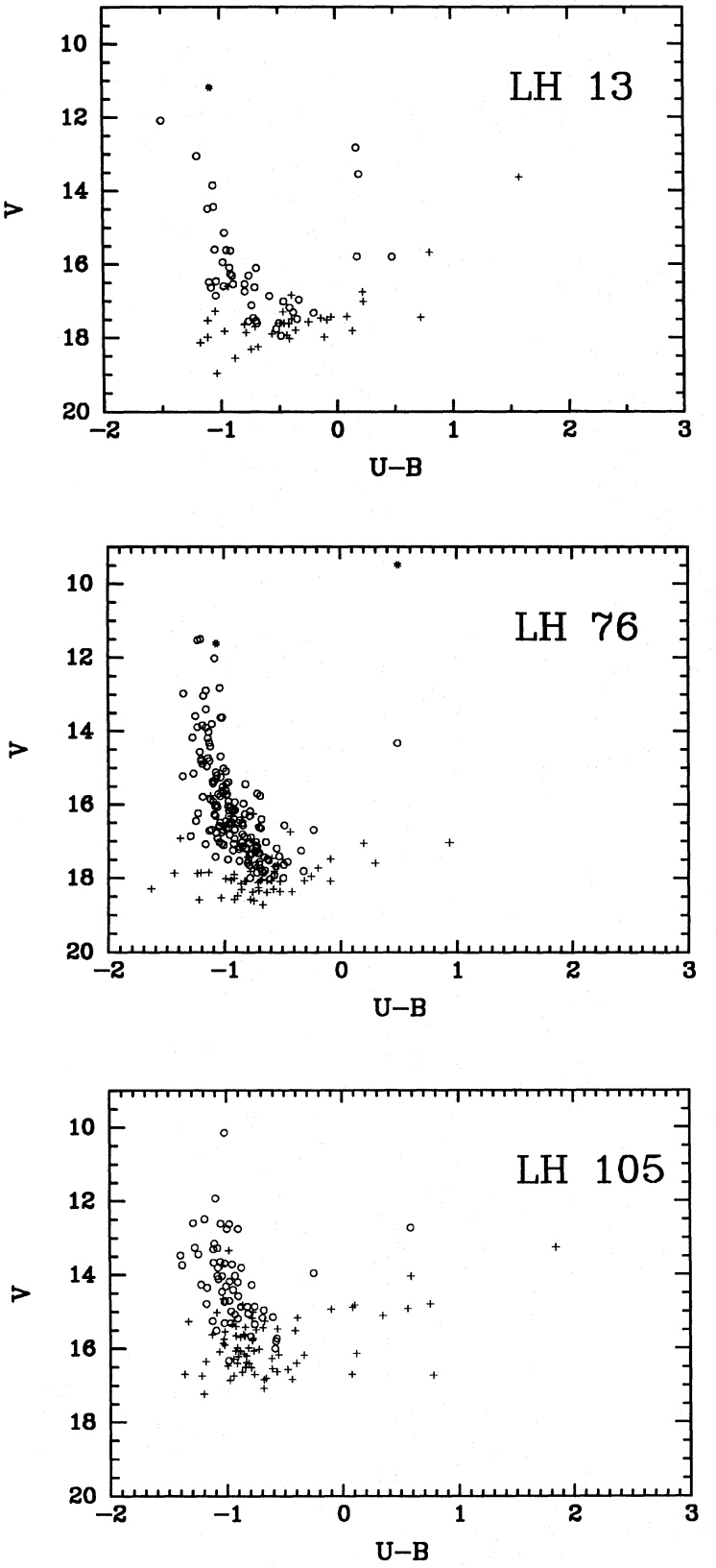


FIG. 11. Dereddened color–magnitude diagrams in $V$ vs $U-B$ for the three regions. The symbols are the same as in Fig. 10.

TABLE 9. Stars taken from the literature.

| Star | $V$ | $B-V$ | $U-B$ |
|---|---|---|---|
| SK-66 41 | 11.69 | −0.12 | −0.97 |
| SK-67 173 | 12.04 | −0.12 | −0.96 |
| SK-67 178a | 9.91 | 1.15 | 0.60 |

spatial distribution of stars with high and low reddenings, and found no clear correlation of the degree of reddening with position.

The photometry for LH 105 is somewhat less precise than the other two regions presented here because only short exposures were taken for this region. However, inspection of Fig. 12 indicates that, even given the poorer photometry, there are many fairly luminous red stars present. We ran a check to determine whether these stars are "real." There are similar stars in the color–magnitude diagram for LH 13, which had both long and short exposures. The red stars in LH 13 did not disappear and the overall scatter did not increase significantly redward when only the short frames were used; thus we do not feel that the red stars in LH 105 are manifestations of the poorer photometry.

Examination of the spatial distribution of the red stars shows that the stars are spread fairly evenly throughout the region. One possibility is that the stars are foreground stars, even though inspection of Fig. 12 shows that this is unlikely. A check of the few stars which were blue enough to have good $U$ magnitudes but still off the main sequence showed that they had very high reddenings; thus it seems even more unlikely that they are foreground stars. Another possibility is that the stars are pre-main sequence; since the reddening is quite high, we might expect LH 105 to be quite young. However, the red stars are not restricted spatially to the knots of nebulosity, which one might expect if they were pre-main sequence.

The most likely explanation, then, is these stars are representative of a slightly older population. Given its location on the outskirts of 30 Doradus, multiple episodes of recent star formation, possibly at slightly different distances, are not unlikely. Inspection of the Hodge–Wright atlas (Hodge & Wright 1967) shows that the density of bright stars south of 30 Dor is higher than in surrounding regions.

### *3.6 Luminosity Functions*

In Fig. 13 we present the luminosity functions for the three associations. We have chosen to present the luminosity functions in dereddened $V$ magnitude rather than observed $V$ magnitude due to the large scatter in the reddenings; it was felt that this scatter might skew the slope of the function. The stars have been "binned" in half magnitude bins as a function of dereddened $V$ magnitude. The solid lines in the step function represent the number of stars with "good" photometry as defined above; the dashed lines indicate the additional numbers of stars with poorer photometry. The three stars added into the color–magnitude diagrams have also been added into the luminosity functions, and are denoted by dotted lines.

Inspection of luminosity functions constructed with observed magnitudes (not shown) rather than dereddened magnitudes shows the functions dropping off at $V=18$ in LH 13, $V=18.5$ in LH 76, and $V=16.5$ in LH 105. The fainter limit in LH 76 can be traced to the better seeing; the brighter limit in LH 105 is expected from the lack of deep exposures.

The typical argument is that the photometry is complete to the magnitude at which the luminosity function drops off. This is a somewhat circular argument, since we do not know that in fact the true luminosity functions do not start to drop off of their own accord. However, for a distance modulus of 18.3, a dereddened $V$ magnitude of 17.5 corresponds to an $M_V$ of −0.8, or roughly a ZAMS B3 star (Panagia 1973). There is no evidence to expect a luminosity function to drop off at so early a spectral type, so we will assume that our photometry is complete to the apparent $V$ magnitudes quoted above.

Mateo (1988) derived luminosity and mass functions for six Magellanic Cloud clusters. In Fig. 14 we present a graphical comparison of the luminosity function of LH 76 to that of NGC 1711, the youngest LMC cluster studied by Mateo (1988). We have chosen LH 76 because it is the most populous of our three associations, and also the one association which has no evidence for contamination from background stars. No vertical scale shifts have been applied to either data set; the data points for LH 76 represent the counts in half-magnitude bins as shown in Fig. 13, except that they have been shifted to fainter magnitudes by the amount dictated by the median reddening, 0.41 mag. Mateo's counts are normalized to the number of stars per square arcminute, and have been corrected for the presence of evolved stars and field stars; the counts shown are taken from his "adopted" column in Table 5. In both cases, the error bars represent $n^{1/2}$, where $n$ is the observed number of stars in each bin. In doing this, we assume that the distribution of star counts is represented by the Poisson distribution.

Mateo found that the mass functions for all six clusters were similar, with some indication that the average mass function was flatter for the high-mass stars than for the low-mass stars. Although the slopes of the luminosity functions in Fig. 14 cannot be directly compared to the slopes of the mass functions, they are consistent with the idea that the distribution of stars is flatter at the high-mass end than at the low-mass end.

## 4. SUMMARY

Using point spread function photometry on $U$, $B$, and $V$ CCD frames, we have presented color–magnitude diagrams and luminosity functions for three OB associations in the LMC. The luminosity functions are a necessary first step toward determining the IMF in these regions. The color–magnitude diagram for LH 76 is very clean, with no hint of noncoevality or contamination by an older popula-

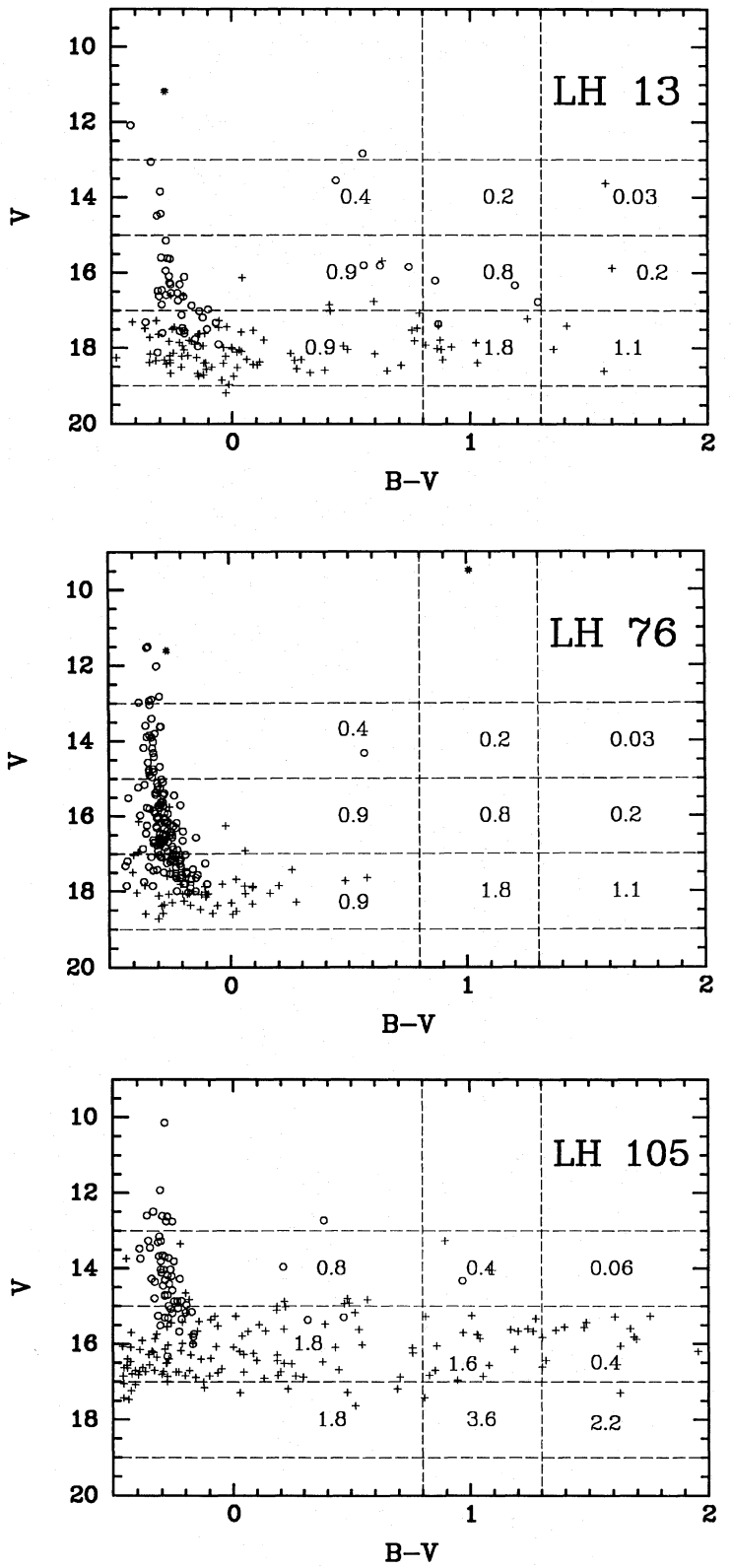


FIG. 12. Dereddened color–magnitude diagrams identical to those in Fig. 10, with the addition of the number of galactic foreground stars predicted by the model of Ratnatunga & Bahcall (1985) for each region of the diagram.

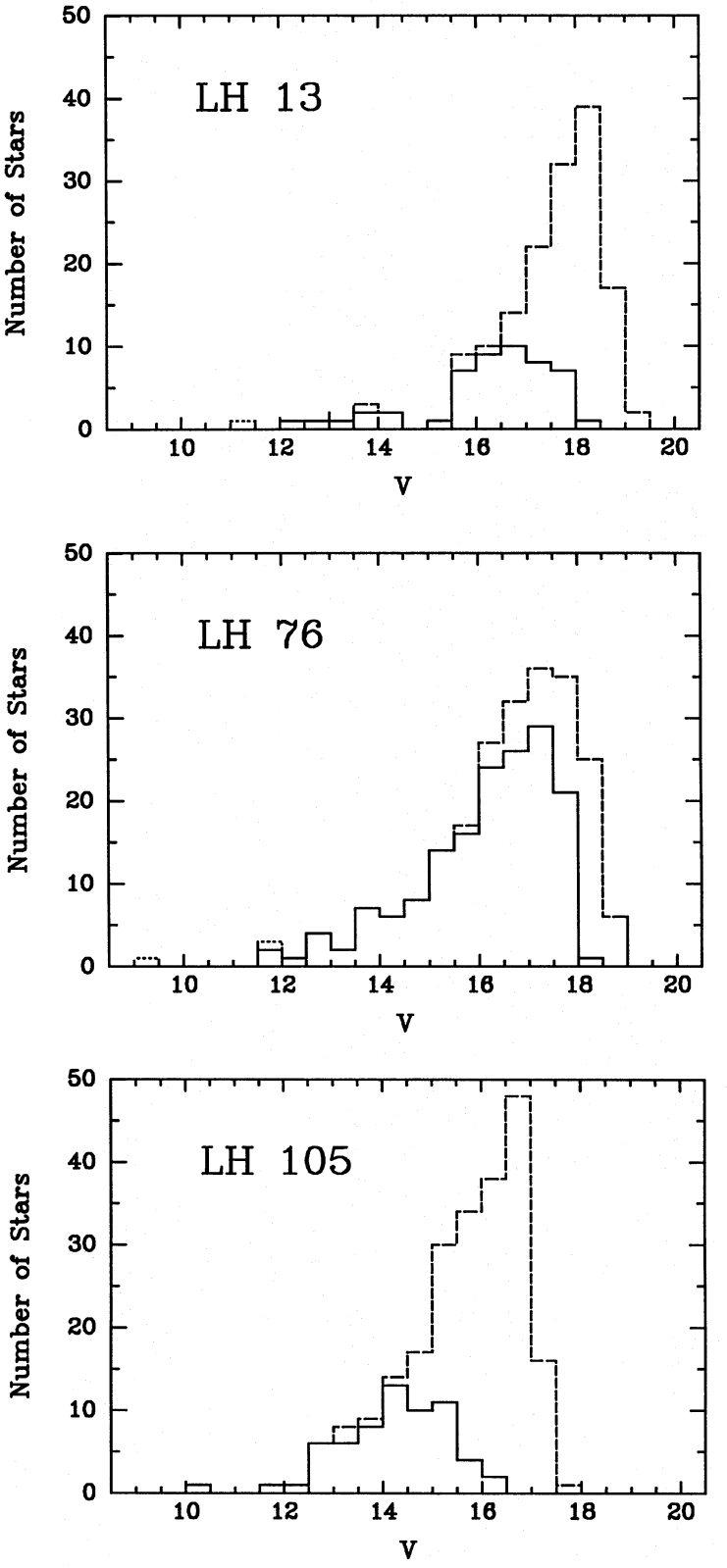


FIG. 13. The luminosity functions as a function of dereddened, apparent $V$ magnitude for the three regions. The histogram shown with solid lines is that obtained using only the stars with "good" photometry as defined in the text; the additional stars shown with dashed lines are the stars with poorer photometry. The dotted lines represent bright stars gleaned from the literature, as discussed in the text.

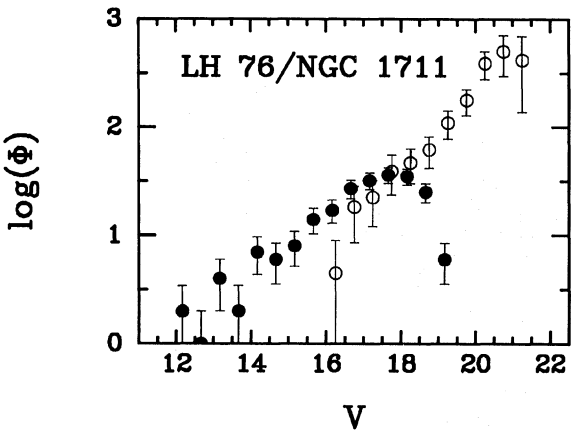


FIG. 14. The luminosity function for LH 76 (filled circles) compared to the luminosity function for NGC 1711 (open circles) from Mateo (1988). The error bars shown indicate $n^{1/2}$, where $n$ is the number of stars in each half-magnitude bin interval. The function for LH 76 is that of Fig. 13, but has been shifted 0.41 mag fainter in accordance with the median reddening.

tion. The luminosity function for LH 76 is compared to that of the youngest cluster studied by Mateo (1988), and is found to be consistent with his observations. The diagram for LH 13 shows some evidence for noncoevality, which can be checked when spectra are used to place the stars on the theoretical H-R diagram. LH 105, which is at the southern edge of the greater 30 Doradus star-forming complex, shows significant contamination by an underlying older population, possibly from previous star forming events.

We would like to thank the wonderfully helpful staff at CTIO, P. Massey with whom these data were obtained as part of a larger collaboration, and the referee, J. Wm. Parker, for useful suggestions. K.D.E. acknowledges the partial support of the NSF under an ROA grant to R. Kennicutt, and from the Northern Arizona University's Organized Research program. R.P.M. acknowledges the support of NASA under the Space Grant program at Northern Arizona University, and D.P.J. the support of the NSF through a Research Experiences for Undergraduates grant to K.D.E. at Northern Arizona University.

## REFERENCES

Bothun, G. 1990, private communication
Cohen, R. S., Dame, T. M., Garay, G., Montani, J., Rubio, M., & Thaddeus, P. 1988, ApJ, 331, L95
Conti, P. S., Garmany, C. D., & Massey, P. 1986, AJ, 92, 48
Cowley, A. P., Crampton, D., & Hutchings, J. B. 1978, AJ, 83, 1619
Davies, R. D., Elliott, K. H., & Meaburn, J. 1976, MRAS, 81, 89
DeGioia-Eastwood, K. 1992, ApJ, 397, 542
Dufour, R. 1984, in Structure and Evolution of the Magellanic Clouds, IAU Symposium No. 108, edited by S. van den Bergh and K. S. de Boer (Reidel, Dordrecht), p. 353
Dufour, R. J., & Duval, J. E. 1975, PASP, 87, 769
Feast, M. W., Thackeray, A. D., & Wesselink, A. J. 1960, MNRAS, 121, 337
Fehrenbach, Ch., Duflot, M., & Duflot 1965, Journ. des Obs. 48, 185
Fitzgerald, M. P. 1970, A&A, 4, 234
Hodge, P. W., & Wright, F. W. 1967, The Large Magellanic Cloud (Smithsonian Publ. No. 4699, Washington, DC)
HST Guide Star Catalog Version 1.1, 1992, Space Telescope Science Institute
Kennicutt, R. C., & Hodge, P. W. 1986, ApJ 306, 130
Koornneef, J. 1984, in Structure and Evolution of the Magellanic Clouds, IAU Symposium No. 108, edited by S. van den Bergh and K. S. de Boer (Reidel, Dordrecht), p. 333
Landolt, A. U. 1983, AJ, 88, 439
Lucke, P. 1972, PhD. thesis, University of Washington
Lucke, P., & Hodge, P. 1970, AJ, 75, 171
Massa, D., & Savage, B. D. 1985, ApJ, 299, 905
Massey, P. 1985, PASP, 97, 5
Massey, P. 1993, in Massive Stars: Their Lives in the Interstellar Medium, edited by J. P. Cassinelli and E. B. Churchwell, p. 168
Massey, P., Garmany, C. D., Silkey, M., & DeGioia-Eastwood, K. 1989, AJ, 97, 107 (Paper I)
Massey, P., & Johnson, J. 1993, AJ (in press)
Massey, P., Parker, J. Wm., & Garmany, C. D. 1989, AJ, 98, 1305 (Paper II)
Massey, P., & Thompson, A. B. 1991, AJ, 101, 1408
Mateo, M. 1988, ApJ, 331, 261
McGee, R. X., Brooks, J. W., & Batchelor, R. A. 1972, AuJPh, 25, 581
Pakull, M. W., & Angebault, L. P. 1987, Nature, 322, 511
Panagia, N. 1973, AJ, 78, 929
Parker, J. Wm. 1991, PASP, 103, 243
Parker, J. Wm., Garmany, C. D., Massey, P., & Walborn, N. 1992, AJ, 103, 1205 (Paper III)
Ratnatunga, K. U., & Bahcall, J. N. 1985, ApJS, 59, 63
Rousseau, J., Martin, N., Prevot, L., Rebeirot, E., Robin, A., & Brunet, J. P. 1978, A&AS, 31, 243
Sanduleak, N. 1969, Contr. CTIO No. 89
Scalo, J. 1986, Fund. Cosmic Phys., 11, 1
Stetson, P. B. 1987, PASP, 99, 191
Walborn, N. 1986, in Luminous Stars and Associations in Galaxies, IAU Symposium No. 116, edited by C. W. H. deLoore, A. J. Willis, and P. Laskarides (Reidel, Dordrecht), p. 185
Wolfire, M. G., & Cassinelli, J. P. 1986, ApJ, 310, 207

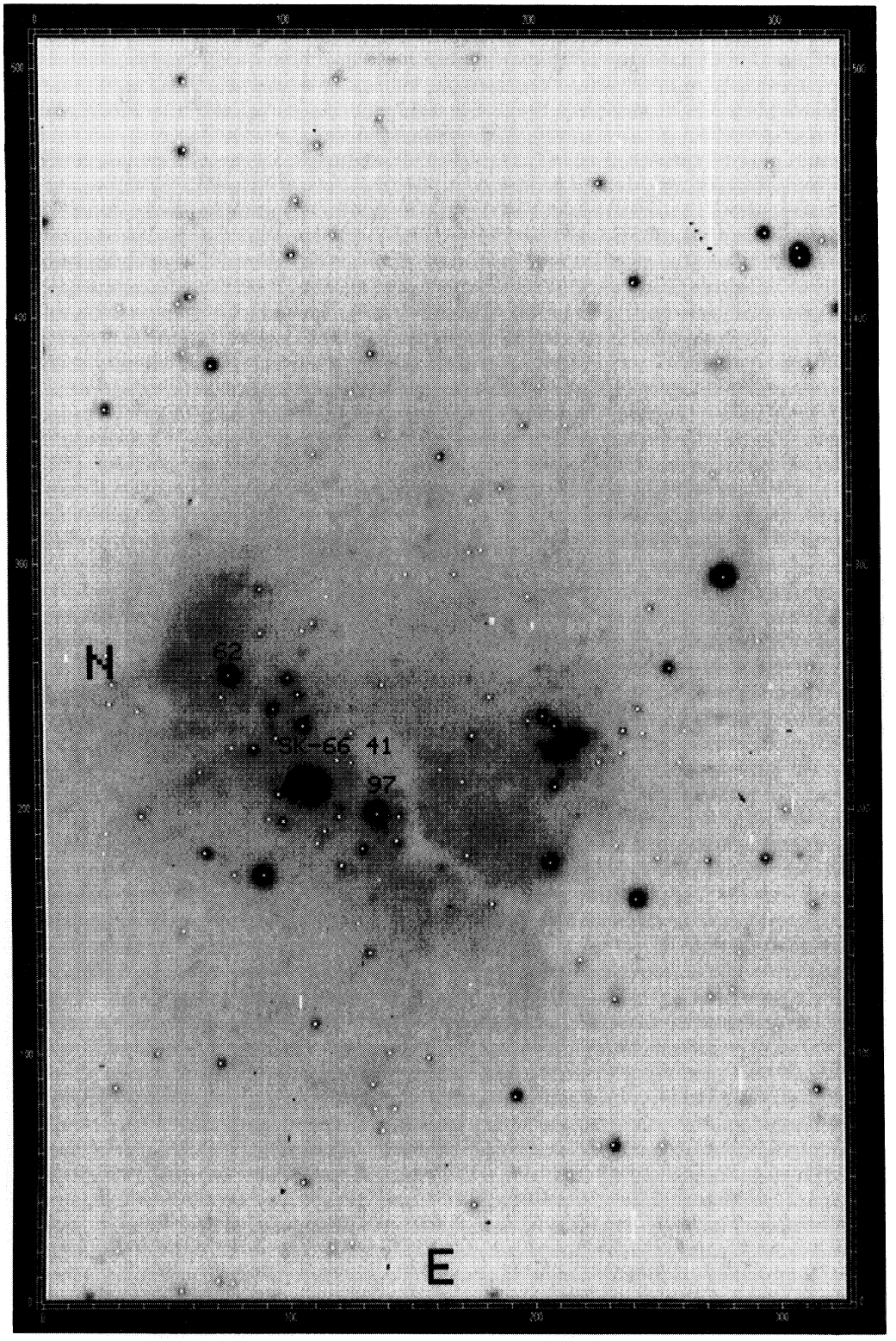


FIG. 1. The longest *V* exposure frame for LH 13; the exposure was 120 s. North is to the left and east is at the bottom.

DeGioia-Eastwood *et al.* (see page 1006)

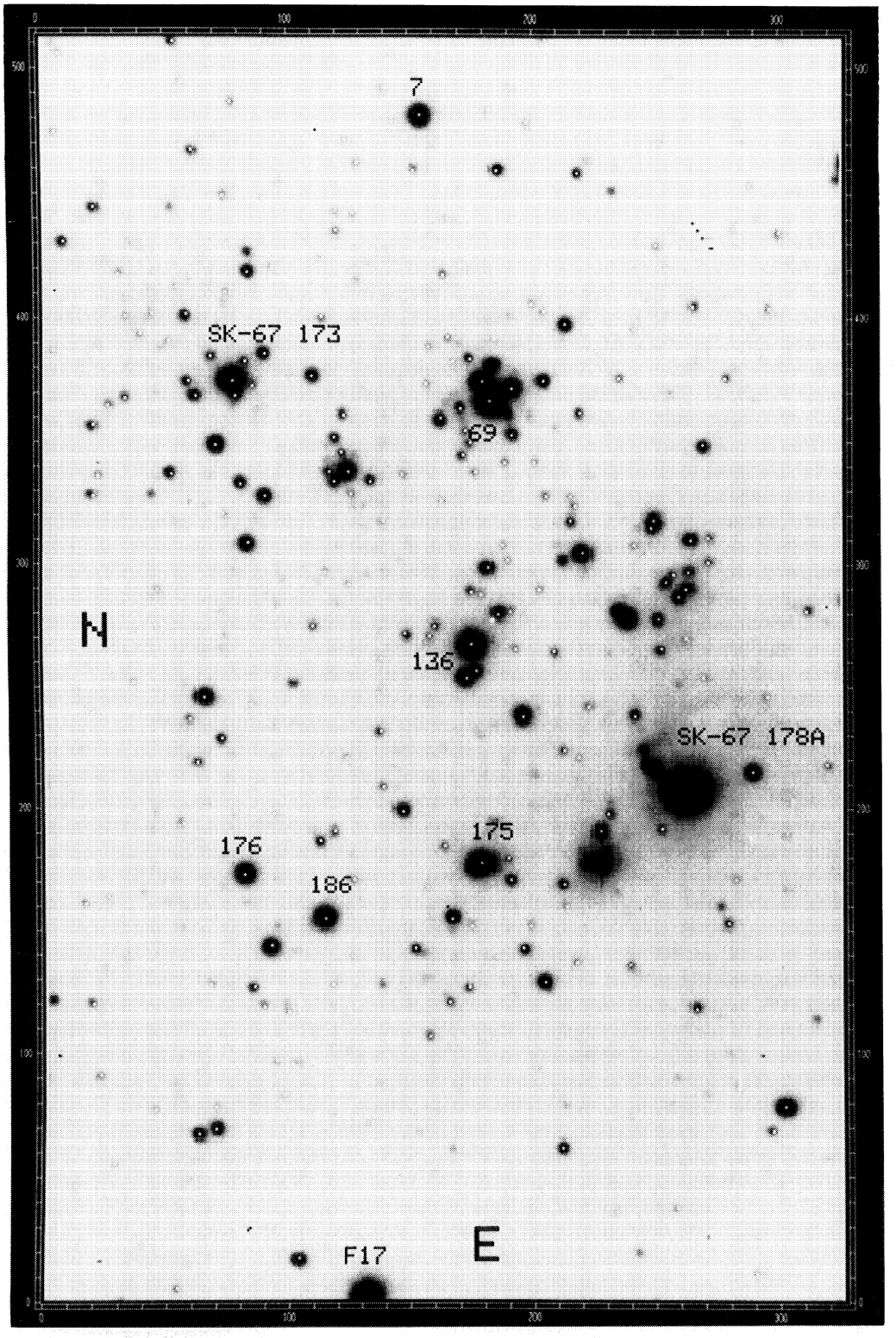


FIG. 2. The longest $V$ exposure frame for LH 76; the exposure was 120 s. North is to the left and east is at the bottom.

DeGioia-Eastwood *et al.* (see page 1006)

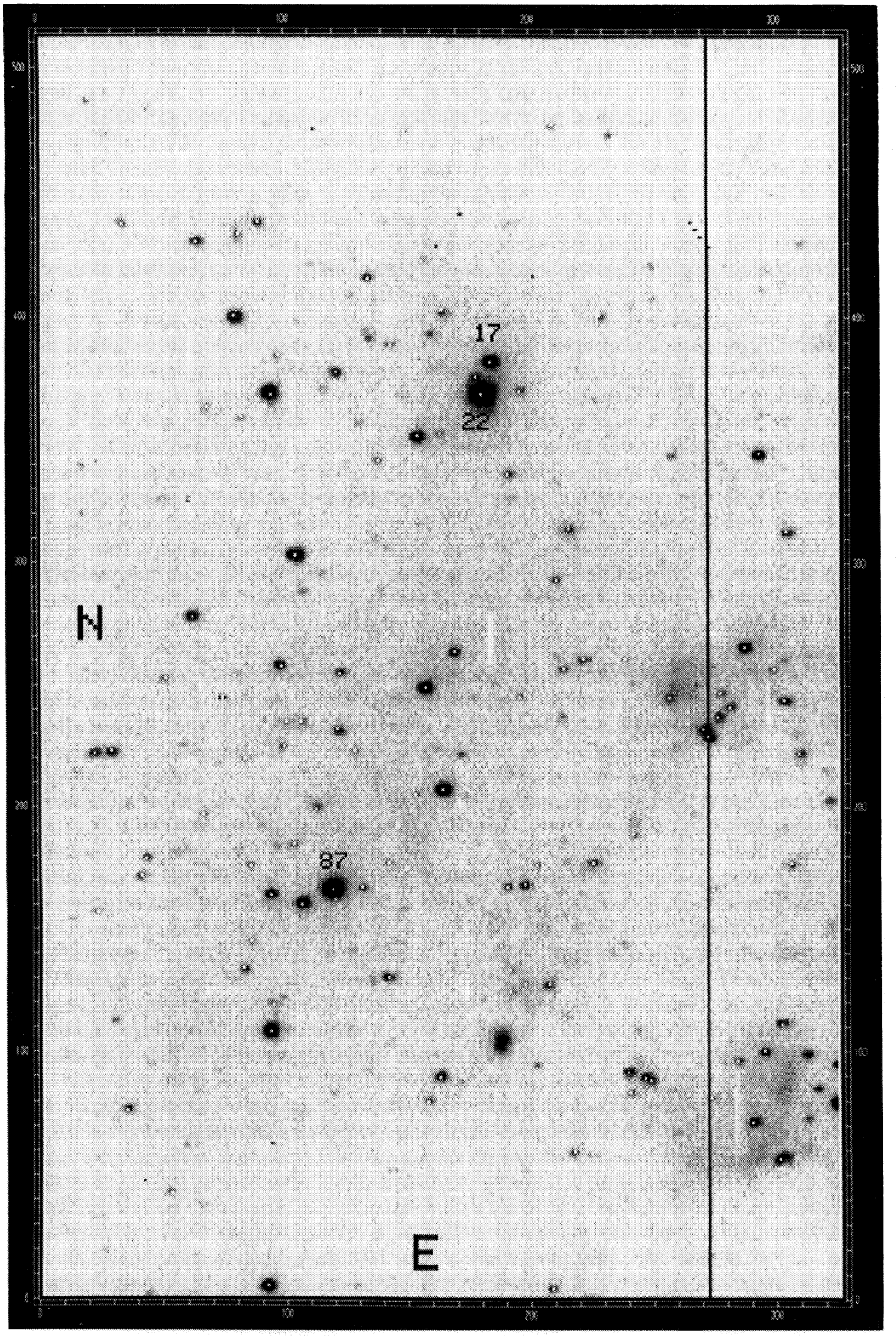


FIG. 3. The *V* frame for the northern region of LH 105; the exposure was 20 s. North is to the left and east is at the bottom.

DeGioia-Eastwood *et al.* (see page 1006)

PLATE 46

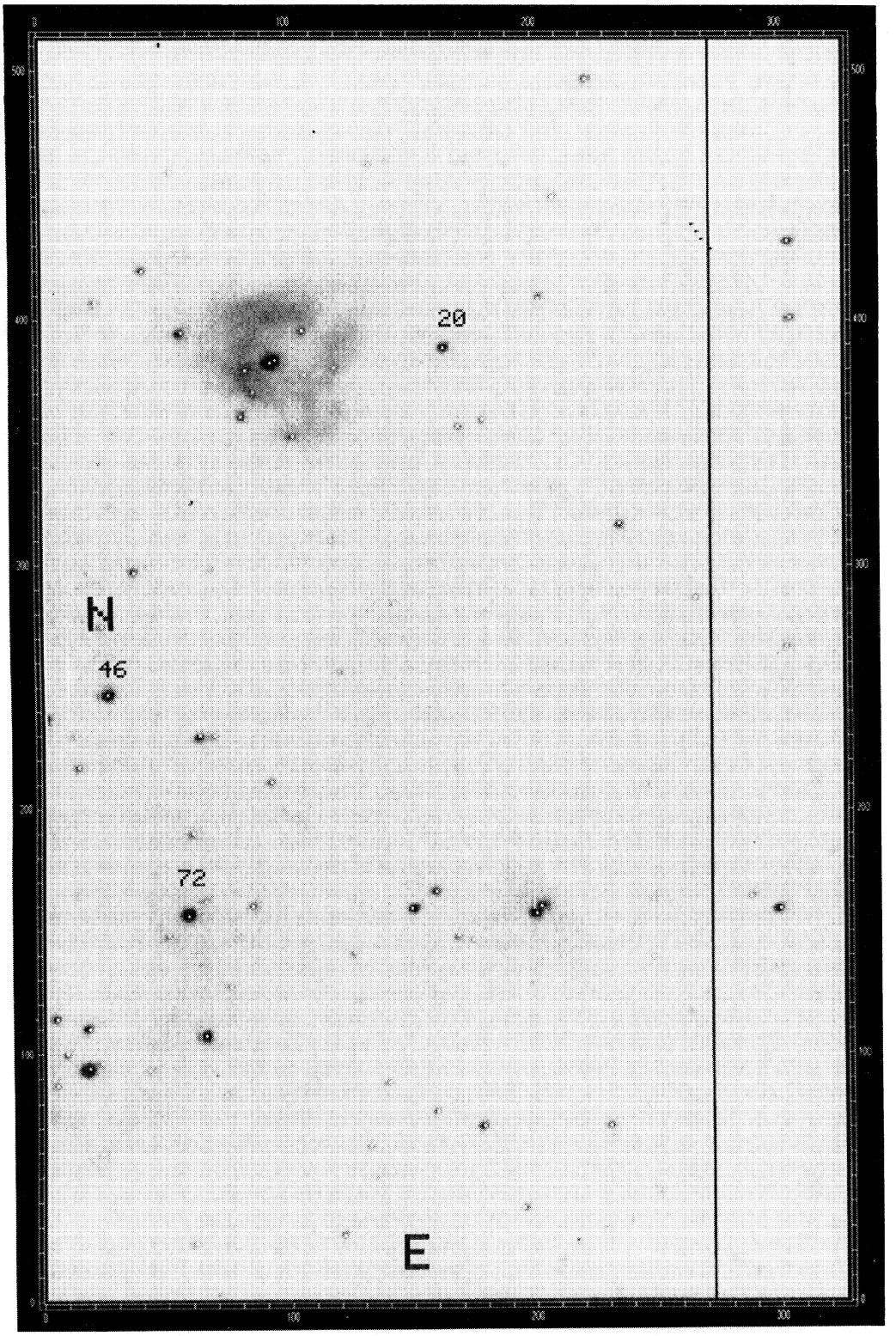


FIG. 4. The *V* frame for the southern region of LH 105; the exposure was 20 s. North is to the left and east is at the bottom.

DeGioia-Eastwood *et al.* (see page 1006)